NATIONAL ADVISORY COMMITTEE FOR AERONAUTICS

TECHNICAL NOTE 3961

EFFECTS OF FUSELAGE NOSE LENGTH AND A CANOPY ON THE STATIC LONGITUDINAL AND LATERAL STABILITY CHARACTERISTICS OF 45° SWEPTBACK AIRPLANE MODELS HAVING FUSELAGES WITH SQUARE CROSS SECTIONS

By Byron M. Jaquet and H. S. Fletcher

Langley Aeronautical Laboratory
Langley Field, Va.

Washington
April 1957

1Q

NATIONAL ADVISORY COMMITTEE FOR AERONAUTICS

TECHNICAL NOTE 3961

EFFECTS OF FUSELAGE NOSE LENGTH AND A CANOPY ON THE STATIC LONGITUDINAL AND LATERAL STABILITY CHARACTERISTICS OF 45° SWEPTBACK AIRPLANE MODELS HAVING FUSELAGES WITH SQUARE CROSS SECTIONS

By Byron M. Jaquet and H. S. Fletcher

SUMMARY

A wind-tunnel investigation was made at low speed in the Langley stability tunnel to determine the effects of fuselage nose length (the fuselage fineness ratio varied from 7.41 to 10.18) and a canopy on the static longitudinal and lateral stability characteristics of a complete model having a fuselage with square cross sections, a 45° sweptback wing of aspect ratio 3 mounted low on the fuselage, and a 45° sweptback horizontal tail of aspect ratio 4 mounted slightly above the wing chord plane. The data were obtained through an angle-of-attack range of -10° to 32° and an angle-of-sideslip range of -24° to 24°.

The results of the investigation have indicated that the static margin at an angle of attack of 0° was decreased by about 0.09 mean aerodynamic chord when the ratio of the fuselage nose length to the maximum depth was increased from 3.80 to 6.58. At small sideslip angles the addition of the canopy to each complete model had essentially no effect on the lift, drag, and pitching-moment coefficients for the angle-of-attack range investigated; however, at large sideslip angles the canopy produced some effect. With approximately the same amount of directional stability at an angle of attack of 0° (obtained by increasing the vertical-tail size in proportion to the fuselage size), an increase in the nose length caused large decreases, at moderate and high angles of attack, in the directional stability of the complete models with the canopy on or off. The canopy reduced the directional stability of the complete models over almost the entire angle-of-attack range for all nose lengths investigated. For the longest fuselage, the model was directionally stable above the stall with the canopy on but very unstable with the canopy off. It was found, for the model having a fineness ratio of 9.26, that these changes in directional stability due to the canopy were associated with favorable and unfavorable sidewash caused by the canopy and that the fuselage caused large decreases with increasing angle of attack in the tail contribution to the directional stability as a result of adverse sidewash at the tail. The wing caused favorable sidewash and a corresponding increase in the contribution of the tail to the directional stability for the entire angle-of-attack range. In comparison with the fuselage and wing effects, the effects of the canopy were of secondary importance except for the case of the longest fuselage above the stall.

INTRODUCTION

The stability derivatives of an airplane are, of course, dependent on the physical characteristics of the design, such as the fuselage shape, wing position, wing aspect ratio, tail aspect ratio, tail position, and duct size. The effects of some of these parameters on the static lateral and longitudinal stability characteristics have been determined for various general research models in references 1 to 4. Certain other airplane parameters which may affect the static lateral and static longitudinal characteristics of airplanes, however, have received little attention in systematic research programs. Two of these are the effect of fuselage nose length and the effect of a canopy.

The purpose of the present investigation, therefore, was to determine the effects of fuselage nose length and a canopy on the static longitudinal and lateral (primarily directional) stability characteristics of a complete model having a fuselage with square cross sections, a 45° sweptback wing of aspect ratio 3 mounted low on the fuselage, and a 45° sweptback horizontal tail of aspect ratio 4 mounted slightly above the wing chord plane. In addition, the effects of fuselage nose length were determined for a wing-fuselage combination. In order to maintain the same amount of directional stability at an angle of attack of 0° for all complete models, the vertical-tail size was increased in proportion to the increase in fuselage nose length. The fuselage fineness ratio varied from 7.41 to 10.18. The effects of the canopy on the tail contribution to the static longitudinal and static directional stability characteristics were determined, with the wing on and off, for the model with a fuselage of fineness ratio 9.26. The effect on the stability characteristics of blunting the fuselage nose of the complete model with a fuselage of fineness ratio 9.26 was also determined.

The investigation covered an angle-of-attack range of -10° to 32° at sideslip angles of 0° and ±5° and an angle-of-sideslip range of -24° to 24° at angles of attack of 0°, 8°, 16°, 24°, and 32°. The test Mach number was 0.13 and the Reynolds number, based on the wing mean aerodynamic chord, was 0.83×10^6.

SYMBOLS

The data presented herein are referred to the stability system of axes shown in figure 1. The moments were measured about the center-of-gravity position shown in figure 2. The symbols and coefficients used herein are defined as follows:

F_L lift, lb

F'_D drag, lb

F_Y side force, lb

M_X rolling moment, ft-lb

M_Y pitching moment, ft-lb

M_Z yawing moment, ft-lb

b span, ft

S total area, sq ft

S_e exposed area, sq ft

c local chord parallel to plane of symmetry, ft

$\bar{c}$ mean aerodynamic chord, $\frac{2}{S}\int_0^{b/2} c^2 dy$, ft

l tail length from $\bar{c}/4$ of wing to $\bar{c}/4$ of tail measured parallel to fuselage reference line, ft

N/h ratio of fuselage nose length to maximum fuselage depth

n fineness ratio

y spanwise distance measured from and perpendicular to plane of symmetry, ft

q dynamic pressure, $\frac{\rho V^2}{2}$, lb/sq ft

ρ mass density of air, slugs/cu ft

V airspeed, ft/sec

α angle of attack of fuselage reference line, deg

β angle of sideslip, deg

σ angle of sidewash, deg

C_L lift coefficient, $\frac{F_L}{qS_w}$

C_D' drag coefficient, $\frac{F_D'}{qS_w}$

C_Y side-force coefficient, $\frac{F_Y}{qS_w}$

C_l rolling-moment coefficient, $\frac{M_X}{qS_w b_w}$

C_m pitching-moment coefficient, $\frac{M_Y}{qS_w \bar{c}_w}$

C_n yawing-moment coefficient, $\frac{M_Z}{qS_w b_w}$

$C_{Y_\beta} = \frac{\partial C_Y}{\partial \beta}$

$C_{n_\beta} = \frac{\partial C_n}{\partial \beta}$

$C_{l_\beta} = \frac{\partial C_l}{\partial \beta}$

The prefix Δ denotes the contribution of the tail assembly (vertical and horizontal) to a given derivative or coefficient.

Subscripts:

f fuselage

h horizontal tail

v vertical tail

w wing

Model component designations:

For convenience, the model configurations are described by a grouping of the following symbols which denote model components:

F fuselage

W wing

V vertical tail

H horizontal tail

C canopy

APPARATUS AND MODELS

The 6- by 6-foot test section (ref. 5) of the Langley stability tunnel was used for the present investigation. The models were mounted on a single support strut which was rigidly attached to a six-component electromechanical balance system.

A drawing of the models is presented as figure 2. The fuselage of fineness ratio 8.34 (45 inches long) was previously used in reference 1. Fuselage coordinates are given in table I.

A different size vertical tail was used with each fuselage in order to provide about the same directional stability for each model at an angle of attack of 0°. One size horizontal tail was common to all models. The canopy dimensions (table II) were selected as average values determined from several present-day fighter-type airplanes. The canopy is located at the same distance from the nose of each fuselage, and thus its distance from the tail assembly varies with the length of the nose of the fuselages. The fuselages of the models were constructed of balsa wood and were covered with fiber glass. The wing had spruce spars perpendicular to the plane of symmetry and was constructed of a fiber-glass bonding agent molded over a laminated balsa core, and the tail assembly was constructed in a like manner but it did not have spars. The wing was mounted in the same low position with respect to the moment center for wing-alone tests as when installed on the fuselages. Details of the present models are given in table III. Photographs of the models are presented as figure 3.

TESTS

Six-component measurements were made for the complete models (FWVH) with the canopy on and off through an angle-of-attack range of -10° to 32° at sideslip angles of 0° and $\pm 5^\circ$. The complete models, with canopy on and off, were also tested through an angle-of-sideslip range of -24° to 24°

at angles of attack of 0°, 8°, 16°, 24°, and 32°. These tests were repeated for the components of the model having the 50-inch-long fuselage with the canopy on and off. The fuselage nose was blunted by removing 3 inches from the nose for a few tests of the complete model having the 50-inch fuselage. With the canopy off, the wing-fuselage combinations employing the 40-, 45-, and 55-inch-long fuselages were tested through the angle-of-attack range at sideslip angles of 0° and ±5°.

All tests were made at a dynamic pressure of 24.9 lb/sq ft, a Mach number of 0.13, and a Reynolds number of 0.83×10^6 based on the mean aerodynamic chord of the wing.

CORRECTIONS

The angle of attack and drag coefficient were corrected for the effects of the jet boundaries by the methods of reference 6, and the tail-on pitching moments were corrected for the effects of jet boundaries by the method of reference 7. The data were not corrected for support-strut interference or blockage effects inasmuch as past experience has shown these corrections to be small or negligible.

RESULTS AND DISCUSSION

The discussion of the static longitudinal stability characteristics will be concerned primarily with the pitching moment and the discussion of the static lateral stability characteristics will be concerned primarily with the yawing moment.

The symbols which appear at the origin of the axes in almost every figure are plotting-machine reference points rather than data points.

Static Longitudinal Stability Characteristics of Complete Models

Effect of fuselage nose length.- An increase in the nose length of the fuselage from 3.80 to 6.58 times the maximum fuselage depth (or width, since the cross section was square) had only a small effect on the lift and drag of the complete model at an angle of sideslip of 0° (fig. 4) for angles of attack below the stall (about 24°). These small effects consisted of increases in these characteristics which began at low angles of attack and occurred with the canopy on or off. The lift and drag were increased somewhat for angles of attack above the stall.

A decrease in the static margin of about 0.09 mean aerodynamic chord occurred at an angle of attack of 0° when the ratio of the fuselage nose length to the maximum depth was increased from 3.80 to 6.58 (fig. 4). This decrease was the result of an increase in the unstable pitching moment of the wing-fuselage combination as the nose length was increased. (See fig. 5.) Inasmuch as the horizontal-tail size was not varied with the fuselage length, the increments in the pitching moment that occurred (fig. 4) would be expected. An examination of the data of figures 4 and 5 indicates very little effect of fuselage nose length on the horizontal-tail contribution to the pitching-moment coefficient. Changes in the fuselage nose length had little effect on the variation of the pitching-moment coefficient with angle of sideslip for angles of attack less than about 16°. (See fig. 6(b).) At higher angles of attack the variation of C_m with β generally became greater with an increase in fuselage nose length.

Effect of canopy.- The canopy had essentially no effect on the lift and drag of the complete model at $\beta = 0°$ (fig. 4) and had a slight effect on the pitching moment only at angles of attack above the stall. In general, the canopy had little effect on the variation of the pitching-moment coefficient with angle of sideslip (fig. 6(b)) for angles of attack below the stall, but at higher angles of attack the canopy generally made the pitching moment more negative and, in some cases, depending on the fuselage nose length, reduced the variation of C_m with β.

Effect of blunt fuselage nose.- In order to simulate the nose shape for a fuselage having a nose inlet, the fuselage of fineness ratio 9.26 was cut perpendicular to the center line at a distance from the nose of 6 percent of the fuselage length (3 inches), and this operation resulted in a fuselage of fineness ratio 8.71. No flow was provided through the fuselage, however. This modification had essentially no effect on the lift, drag, and pitching-moment characteristics of the complete model (fig. 7), and a comparison of figures 6(b) and 8(a) indicates little effect of the modification on the variation of the pitching-moment coefficient with angle of sideslip.

Effect of Components on Tail Contribution to Static Longitudinal Stability Characteristics

The model having a fuselage of fineness ratio 9.26 was selected for breakdown tests to determine the effects of the model components on the contribution of the tail assembly (vertical and horizontal) to the pitching-moment coefficient.

Effect of canopy on tail contribution to C_m.- An examination of the data of figure 9 at $\beta = 0°$ indicates that, with the wing off, the canopy

produced essentially no change in the contribution of the tail to the pitching-moment coefficient of the model as expressed by the curves FVH - F and FVHC - FC. With the wing on, the canopy produces a small negative increment in the tail contribution to the pitching-moment coefficient as expressed by the curves FWVH - FW and FWVHC - FWC.

The variation of the tail contribution to the pitching-moment coefficient (ΔC_m) with angle of sideslip is affected only slightly by the canopy with the wing off. (See fig. 10.) With the wing on, the canopy generally caused a greater variation of ΔC_m with β at the high angles of attack. The tail-contribution data of figure 10 were determined from the data of figures 11 and 12.

Effect of wing on tail contribution to C_m.- The addition of the wing (fig. 9) in the low position to the fuselage reduced the contribution of the tail to the pitching-moment coefficient at $\beta = 0^\circ$ for the low and moderate angle-of-attack ranges and increased the tail contribution at high angles of attack. The variation of $-\Delta C_m$ with β was changed considerably by the addition of the wing. (See fig. 10.) With the wing off, positive increments of ΔC_m occurred when the value of $-\beta$ was changed from 0°. With the wing on, however, positive increments were obtained only at the angles of attack beyond the stall and at these angles the variation of ΔC_m with β was much larger with the wing on than with the wing off. At the lower angles of attack with the wing on, the values of ΔC_m generally became more negative when β was changed from 0°.

Static Longitudinal Stability Characteristics of Wing

In order to determine the characteristics of the wing alone in the same low position with respect to the moment center as when used on the fuselage, it was tested installed on the strut as shown in figure 3. The pitching-moment coefficient of the wing did not vary appreciably with angle of attack (fig. 9) and the wing was essentially neutrally stable at low angles of attack. Maximum lift of the wing was achieved at an angle of attack of 24.5° and at this angle of attack the greatest variation of C_m with β occurred. (See fig. 13.)

Static Lateral Stability Characteristics

Effect of fuselage nose length.- When the fuselage nose length was increased, the vertical-tail size was also increased in order to maintain approximately the same amount of directional stability at an angle of attack of 0°. It would therefore be expected that, because of side-area increases (increased nose area and vertical-tail area) which occur with

an increase in fuselage nose length, the side-force parameter C_{Y_β} would also increase (become more negative) and this fact is indicated by the data of figure 14.

At moderate and high angles of attack an increase in the fuselage nose length (fig. 14) resulted in large changes in the directional stability of the complete model with the canopy on or off. The complete model with the shortest fuselages (fineness ratios of 7.41 and 8.34) and without the canopy had directional stability throughout the angle-of-attack range investigated. With the canopy, however, there was some degree of directional instability in the high angle-of-attack range for all models. The complete model with the longest fuselage became directionally unstable earlier than the other models (canopy on or off). An increase in the directional instability of the wing-fuselage combination with an increase in fuselage nose length for almost the entire angle-of-attack range (fig. 15), together with the rapid decrease with increasing angle of attack in the vertical-tail contribution to directional stability (fig. 16), accounts for the rapid decrease in directional stability of the complete model with increasing angle of attack (fig. 14). At low angles of attack the instability of the wing-fuselage combination varied linearly with fuselage nose length. At high angles of attack the longest wing-fuselage combination became very unstable (fig. 15), and, since there was little change in the tail contribution in this region (fig. 16), this instability accounts for the large amount of instability for the complete model with the longest nose (fig. 14). In the low angle-of-attack range there is, of course, an increase in the vertical-tail contribution inasmuch as the tail size was varied in proportion to the fuselage nose length; but, as mentioned previously, each tail contribution decreased with increasing angle of attack (fig. 16). Only the tail contribution for the longest fuselage, however, decreased to zero and this occurred above the stall. When normalized with respect to the value of ΔC_{n_β} (for each nose length) at $\alpha = 0^\circ$, little systematic effect of nose length is noted although the tail contribution for the longest nose length decreases more rapidly than the others at moderate angles of attack. (See fig. 16.) If the vertical tail span were held constant when the nose length was changed, instead of being varied as was done herein, a greater effect of nose length on the directional stability might have been obtained owing to the relative location of the fuselage vortices with respect to the vertical tail. For the present investigation, with the vertical-tail span being changed in proportion to the fuselage nose length, the fuselage vortices would be expected to remain in essentially the same relative position with respect to the vertical tail for all nose lengths. In figure 17 the tail contribution for each configuration can be seen with respect to the wing-fuselage combination and the complete model. It should be noted that the data for the wing-fuselage combination were obtained with the canopy off only.

At angles of attack beyond the stall the trends become erratic, probably because of nonlinearities in the curves of the coefficients plotted against angle of sideslip (see figs. 6(d) to 6(f), for example); therefore, caution should be exercised in the use of the stability derivatives in the high angle-of-attack range.

The variation of C_n with β (fig. 6(f)) was essentially linear for angles of attack below the stall (about 24°) for the complete model with the shortest fuselage. At higher angles of attack the curve of C_n against β is nonlinear and at an angle of attack of 32.7° directional instability as well as the nonlinearity occurred at small angles of sideslip. An increase in the fuselage nose length (for the complete model) resulted in a greater variation of C_n with β, an increase in directional instability, and an earlier departure of the curves from linearity.

Effect of canopy.- For a given fuselage nose length and for angles of attack below the stall (fig. 17), the canopy had no effect on the value of C_{Y_β}. In all cases at angles of attack above the stall, C_{Y_β} became less negative when the canopy was added. Except for the longest fuselage nose length investigated, the canopy reduced the directional stability of the complete model over the entire angle-of-attack range. For the longest fuselage, the model was directionally stable at angles of attack above the stall with the canopy but very unstable without the canopy (fig. 17(d)). The canopy also affected the nature and magnitude of the variation of C_n with β, the degree of the effects depending on the angle of attack and fuselage nose length but, in general, the curves became less linear when the canopy was on the models.

Effect of blunt fuselage nose.- Except for angles of attack beyond the stall, blunting the nose of the fuselage of fineness ratio 9.26 improved the directional stability of the complete model (fig. 17(c)), probably as a result of a decrease in the directional instability of the fuselage. At angles of attack above the stall and with the canopy off, directional instability was caused by the blunt nose. In this angle-of-attack region very nonlinear curves of C_n plotted against β were indicated from the data of figure 8(c) and because of this nonlinearity the slopes shown in figure 17(c) at these high angles of attack probably do not truly represent the directional stability of the models.

Effect of Components on Tail Contribution to Static Lateral Stability Characteristics

The model having a fuselage of fineness ratio 9.26 was selected for breakdown tests to determine the effects of the model components on the contribution of the tail assembly (vertical and horizontal) to the static lateral stability (primarily directional) characteristics.

Effect of canopy on the sidewash parameter and on the tail contribution to C_{n_β} and C_n.- The sidewash parameter $\left(1 + \frac{\partial\sigma}{\partial\beta}\right)\frac{q_v}{q}$ which is presented in figure 18 was determined from the side-force parameter C_{Y_β} of figure 19 by the method of reference 2. Since tests of the tail alone were not made for the present investigation, these data were obtained from reference 1. It was necessary, however, to adjust the data of reference 1 to account for the difference in size of the vertical tails. Although the horizontal tail used herein and that of reference 1 were of different aspect ratio (4.00 and 2.77, respectively), the theoretical investigation of reference 8 indicated no effect of this difference on the side-force parameter of the vertical tail at low angles of attack, and, accordingly, no additional adjustment was made to the data to account for the difference in the horizontal-tail aspect ratio. The experimental investigation of reference 9 also indicates little effect of this small difference in horizontal-tail aspect ratio on the derivative C_{Y_β} at an angle of attack of 0°. In the high angle-of-attack range, it is not known whether appreciable differences in the value of C_{Y_β} would occur owing to the difference in the horizontal-tail aspect ratio used in reference 1 and that of the present investigation.

The data of figure 18 indicate that with the wing off and the canopy off a large increase in the adverse sidewash occurs as the angle of attack is increased, and, for angles of attack greater than 19°, the adverse sidewash becomes so great that the contribution of the vertical tail becomes unstable. Corresponding decreases in the tail contribution are associated with the unfavorable changes in sidewash at the tail. The addition of the wing provides a favorable change in sidewash and in the tail contribution to the directional stability throughout the angle-of-attack range (fig. 18). In comparison with the fuselage and wing effects, the effects of the canopy were of secondary importance except for the case of the longest fuselage above the stall.

Additional adverse sidewash at the tail was caused by the canopy (fig. 18) for all angles of attack except near the stall. This adverse sidewash resulted in a decrease in the tail contribution to the directional stability $\left(\Delta C_{n_\beta}\right)$ in this angle-of-attack range. In the region of the stall the canopy produced favorable sidewash at the tail and this, of course, slightly increased ΔC_{n_β}. These effects of the canopy were similar with the wing on and off.

Since the sidewash data, which were determined with isolated-tail data for a horizontal tail of aspect ratio 2.77 instead of 4.00 as used herein, adequately describe the tail contribution to C_{n_β} in the high angle-of-attack range, it would appear that the difference in horizontal-tail aspect ratio between the model used herein and the model of reference 1 was of little consequence with regard to the derivative C_{Y_β}.

The nonlinearities that occur at high angles of attack in the variation of the coefficients with angle of sideslip (see figs. 6(d) to 6(f), for example) should be considered when the stability derivatives are used for that angle-of-attack range. In the high sideslip-angle range (fig. 20) the canopy also generally had an adverse effect on the contribution of the tail to the yawing-moment coefficient (ΔC_n), especially at angles of attack near and above the stall.

Effect of wing on sidewash parameter and on tail contribution to C_{n_β} and C_n.- The addition of the wing in the low position to the fuselages (fig. 18) produced favorable sidewash at the tail, canopy on or off, for almost the entire angle-of-attack range. (An exception was with the canopy off at angles of attack above 30°.) Corresponding increases in the tail contribution to the directional stability due to the wing were apparent from the data of figure 18. With the wing on the tail contributed positive directional stability for the entire angle-of-attack range, whereas with the wing off the tail contribution became zero at an angle of attack below the stall. The favorable sidewash due to the addition of the wing is in agreement with the investigation of reference 10 wherein, for a fuselage with square cross sections, the addition of swept or unswept wings in the low or high positions contributed favorable sidewash at the tail, the greatest amount of favorable sidewash being contributed by the low wing positions.

Effect of canopy on fuselage and wing-fuselage characteristics.- As would be expected, the addition of the canopy to the fuselage resulted in greater directional instability in the low angle-of-attack range. (See fig. 19.) For higher angles of attack, however, the canopy decreased the instability of the fuselage. Also, for angles of attack above about 30°, the fuselage with the canopy became directionally stable. The addition of the canopy to the wing-fuselage combination results in more instability throughout the angle-of-attack range with the greatest effect of the canopy occurring at angles of attack above the stall.

CONCLUSIONS

An investigation made at low speed in the Langley stability tunnel to determine the effects of fuselage nose length (the fuselage fineness ratio varied from 7.41 to 10.18) and a canopy on the static longitudinal and lateral stability characteristics of an airplane model having a low-mounted 45° sweptback wing of aspect ratio 3, a 45° sweptback horizontal tail of aspect ratio 4 mounted slightly above the wing chord plane, and square fuselage cross sections has indicated the following conclusions:

1. An increase in the ratio of the fuselage nose length to the maximum depth from 3.80 to 6.58 reduced the static margin at an angle of attack of 0° by about 0.09 mean aerodynamic chord, had little effect on the lift below the stall, and increased the lift somewhat for angles of attack above the stall.

2. The addition of the canopy to the models had essentially no effect on lift, drag, and pitching moment for the angle-of-attack range investigated.

3. With approximately the same amount of directional stability at an angle of attack of 0° (obtained by increasing the vertical-tail size in proportion to the fuselage size), an increase in the fuselage nose length caused a large decrease in the directional stability of the complete model with canopy on or off at moderate and high angles of attack. This large decrease was caused by an increase in the directional instability of the wing-fuselage combination with an increase in fuselage nose length together with the rapid decrease in the vertical-tail contribution to directional stability. Only complete models having fuselages of fineness ratio 7.41 and 8.34 and without the canopy had directional stability throughout the angle-of-attack range.

4. Except for the longest fuselage length investigated, the canopy reduced the directional stability of the complete models over the entire angle-of-attack range. For the longest fuselage, the model was directionally stable above the stall with the canopy on but very unstable with the canopy off.

5. The results of breakdown tests, made only for the model having a fuselage of fineness ratio 9.26, indicated that adverse sidewash at the tail coming from the fuselage caused the contribution of the vertical-horizontal tail assembly to deteriorate rapidly as the angle of attack was increased so that at angles of attack beyond the stall the tail contribution became unstable. The addition of the low wing of aspect ratio 3 caused favorable sidewash throughout the angle-of-attack range and this sidewash resulted in an increase in the tail contribution. The canopy also caused adverse sidewash (the effect of the canopy was secondary to the wing and fuselage effects except for the case of the longest fuselage above the stall) and a corresponding decrease in the tail contribution for all angles of attack except near the stall where favorable sidewash and a slight increase in the tail contribution resulted from the canopy.

Langley Aeronautical Laboratory,
National Advisory Committee for Aeronautics,
Langley Field, Va., January 24, 1957.

REFERENCES

1. Letko, William, and Williams, James L.: Experimental Investigation at Low Speed of Effects of Fuselage Cross Section on Static Longitudinal and Lateral Stability Characteristics of Models Having 0° and 45° Sweptback Surfaces. NACA TN 3551, 1955.

2. Goodman, Alex, and Thomas, David F., Jr.: Effects of Wing Position and Fuselage Size on the Low-Speed Static and Rolling Stability Characteristics of a Delta-Wing Model. NACA Rep. 1224, 1955. (Supersedes NACA TN 3063.)

3. Wolhart, Walter D., and Thomas, David F., Jr.: Static Longitudinal and Lateral Stability Characteristics at Low Speed of Unswept-Midwing Models Having Wings With an Aspect Ratio of 2, 4, or 6. NACA TN 3649, 1956.

4. Jaquet, Byron M., and Williams, James L.: Wind-Tunnel Investigation at Low Speed of Effect of Size and Position of Closed Air Ducts on Static Longitudinal and Static Lateral Stability Characteristics of Unswept-Midwing Models Having Wings of Aspect Ratio 2, 4, and 6. NACA TN 3481, 1955.

5. Bird, John D., Jaquet, Byron M., and Cowan, John W.: Effect of Fuselage and Tail Surfaces on Low-Speed Yawing Characteristics of a Swept-Wing Model As Determined in Curved-Flow Test Section of Langley Stability Tunnel. NACA TN 2483, 1951. (Supersedes NACA RM L8G13.)

6. Silverstein, Abe, and White, James A.: Wind-Tunnel Interference With Particular Reference to Off-Center Positions of the Wing and to the Downwash at the Tail. NACA Rep. 547, 1936.

7. Gillis, Clarence L., Polhamus, Edward C., and Gray, Joseph L., Jr.: Charts for Determining Jet-Boundary Corrections for Complete Models in 7- by 10-Foot Closed Rectangular Wind Tunnels. NACA WR L-123, 1945. (Formerly NACA ARR L5G31.)

8. Queijo, M. J., and Riley, Donald R.: Calculated Subsonic Span Loads and Resulting Stability Derivatives of Unswept and 45° Sweptback Tail Surfaces in Sideslip and in Steady Roll. NACA TN 3245, 1954.

9. Riley, Donald R.: Effect of Horizontal-Tail Span and Vertical Location on the Aerodynamic Characteristics of an Unswept Tail Assembly in Sideslip. NACA Rep. 1171, 1954. (Supersedes NACA TN 2907.)

10. Letko, William: Experimental Investigation at Low Speed of the Effects of Wing Position on the Static Stability of Models Having Fuselages of Various Cross Section and Unswept and 45° Sweptback Surfaces. NACA TN 3857, 1956.

TABLE I.- FUSELAGE COORDINATES

Fuselage of fineness ratio 7.41

x/l_f	w/l_f
0	0
.05	.015
.10	.027
.15	.038
.20	.047
.25	.054
.30	.060
.35	.064
.40	.067
.45	.068
.50	.066
.55	.065
.60	.063
.65	.060
.70	.057
.75	.054
.80	.050
.85	.047
.90	.043
.95	.039
1.00	.034

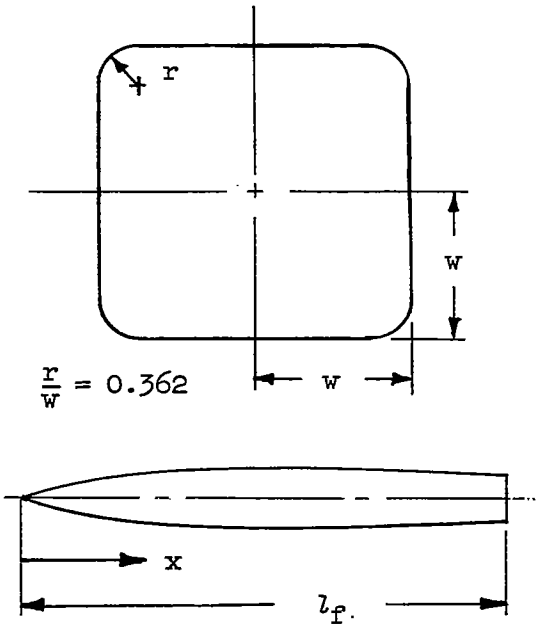

In order to construct the three longer fuselages, sections having a constant cross-sectional area and lengths of 5, 10, and 15 inches were added forward of and beginning at the center of gravity of the small fuselage.

TABLE II.- CANOPY COORDINATES

x/l_c	y/l_c	z/l_c
0	0	0.108
0.018	0.025 0	0.111 .122
0.036	0.032 0	0.114 .136
0.071	0.046 .039 .031 .021 0	0.121 .132 .143 .154 .164
0.143	0.063 0	0.134 .211
0.214	0.073 .066 .059 .049 .038 .024 0	0.145 .161 .179 .196 .214 .232 .241
0.286	0.079 0	0.155 .259
0.357	0.082 0	0.164 .269
0.429	0.084 .080 .071 .061 .051 .036 .014 0	0.171 .179 .196 .214 .232 .250 .268 .271
0.500	0.081 0	0.179 .268
0.571	0.073 0	0.183 .261
0.643	0.063 .057 .046 .032 .009 0	0.186 .196 .214 .232 .250 .252
0.714	0.052 0	0.190 .241
0.786	0.039 0	0.191 .229
0.857	0.026 .019 .016 .006 0	0.193 .200 .207 .214 .216
0.928	0.013 0	0.193 .204
1.000	0	0.193

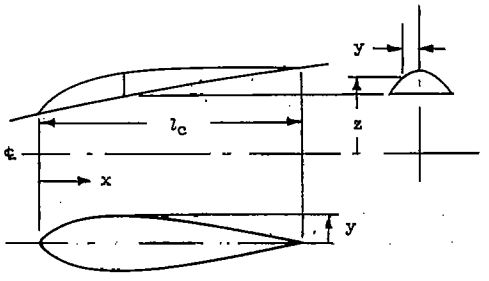

TABLE III.- PERTINENT DETAILS OF MODELS

Fuselage:				
Length, in.	40	45	50	55
Ratio of nose length to afterbody length	1.051	1.308	1.563	1.820
Maximum height and width, in.	5.40	5.40	5.40	5.40
Fineness ratio	7.41	8.34	9.26	10.18
Side area, sq in.	158.7	185.7	212.7	239.7
Volume, cu in.	681.6	823.0	964.4	1105.8
Maximum cross-sectional area, sq in.	28.3	28.3	28.3	28.3
Vertical tail:				
Total area to fuselage center line, S_V, sq in.	48.6	59.0	68.7	79.1
Exposed area, $S_{e,v}$, sq in.	37.0	46.1	54.5	64.0
Span from fuselage center line, in.	8.25	9.09	9.81	10.52
Root chord, in.	7.37	8.11	8.76	9.40
Mean aerodynamic chord, in.	6.03	6.64	7.17	7.69
Sweepback of quarter-chord line, deg	45	45	45	45
Taper ratio	0.6	0.6	0.6	0.6
Aspect ratio	1.4	1.4	1.4	1.4
NACA airfoil section parallel to root chord	65A008	65A008	65A008	65A008
Tail volume, $\frac{l_V S_V}{b_W S_W}$	0.0804	0.0976	0.1136	0.1308
Canopy:				
Length, in.	14.00			
Side area, sq in.	11.9			
Maximum cross-sectional area, sq in.	2.0			
Volume, cu in.	15.1			
Ratio of length to maximum width	5.99			
Ratio of distance from fuselage nose to fuselage width	1.11			
Wing:				
Area, S_W, sq in.	324.0			
Span, in.	31.18			
Root chord, in.	12.99			
Mean aerodynamic chord, in.	10.63			
Sweepback of quarter-chord line, deg	45			
Taper ratio	0.6			
Aspect ratio	3			
NACA airfoil section parallel to plane of symmetry	65A008			
Horizontal tail:				
Total area, S_h, sq in.	64.8			
Span, in.	16.10			
Root chord, in.	5.03			
Mean aerodynamic chord, in.	4.11			
Sweepback of quarter-chord line, deg	45			
Angle of incidence, deg	0			
Dihedral angle, deg	0			
Taper ratio	0.6			
Aspect ratio	4.00			
NACA airfoil section parallel to plane of symmetry	65A008			
Tail volume, $\frac{l_h S_h}{\bar{c}_W S_W}$	0.324			

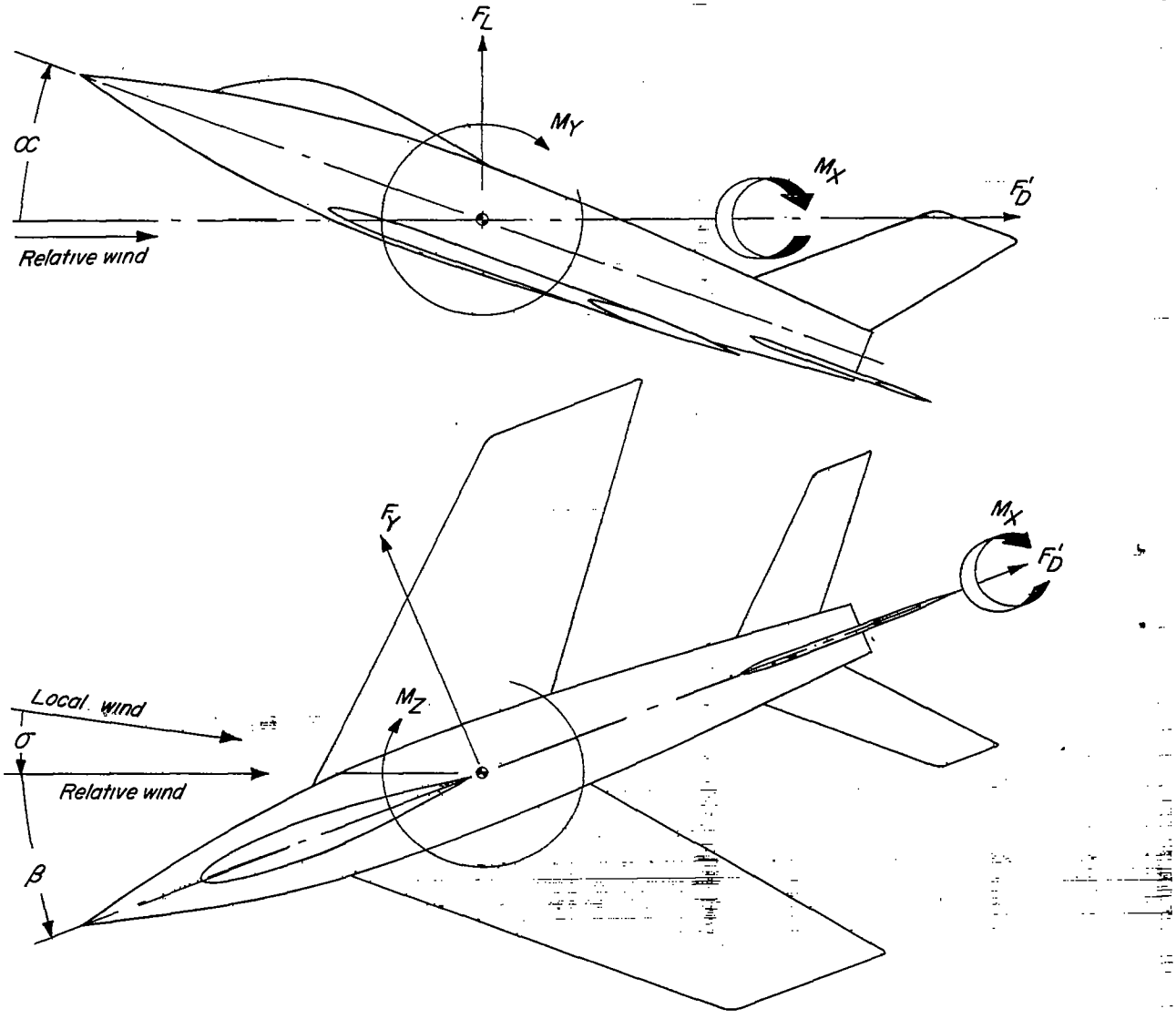

Figure 1.- Stability system of axes. Arrows indicate positive forces, moments, and angular displacements.

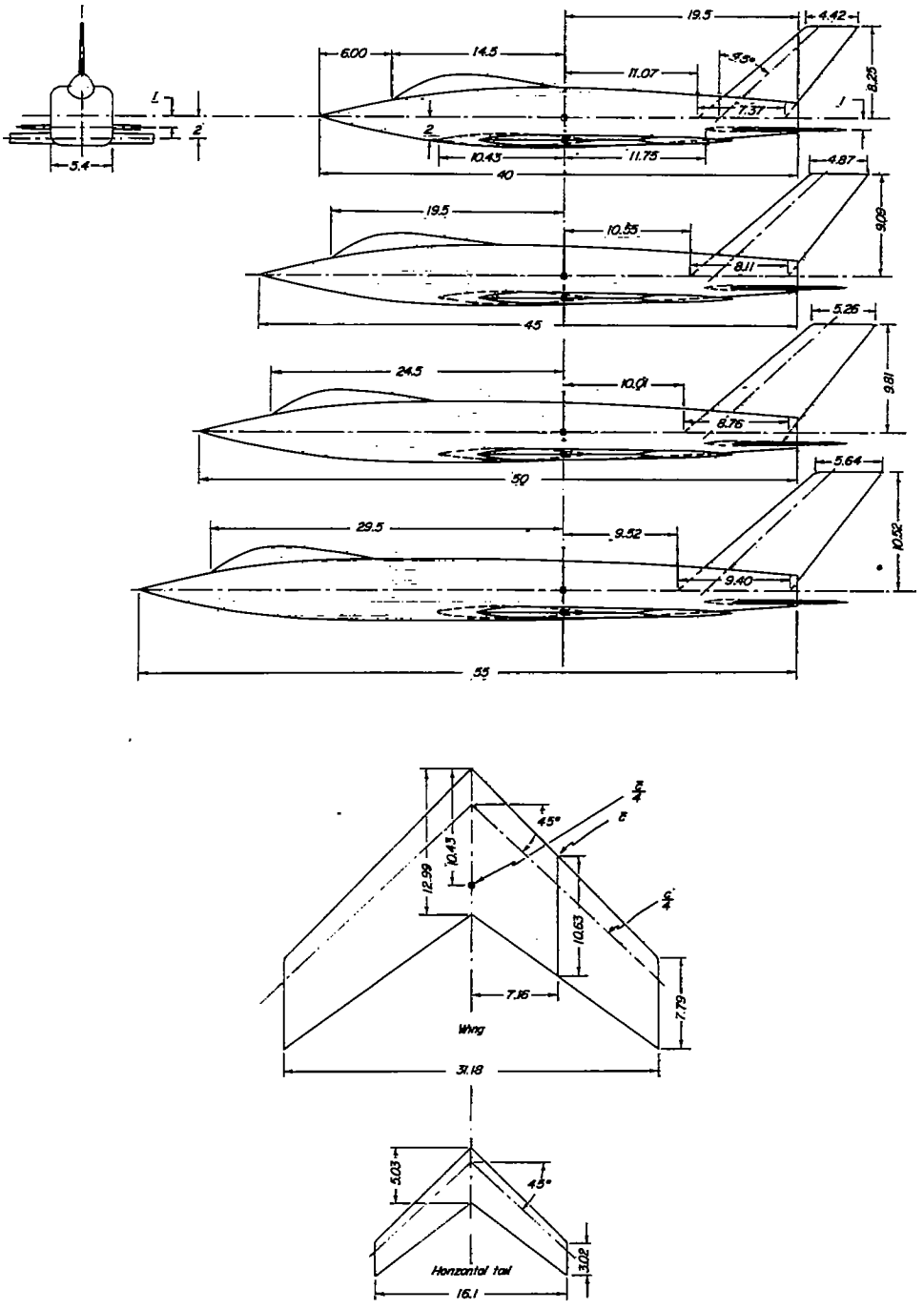

Figure 2.- Details of models. Dimensions are in inches.

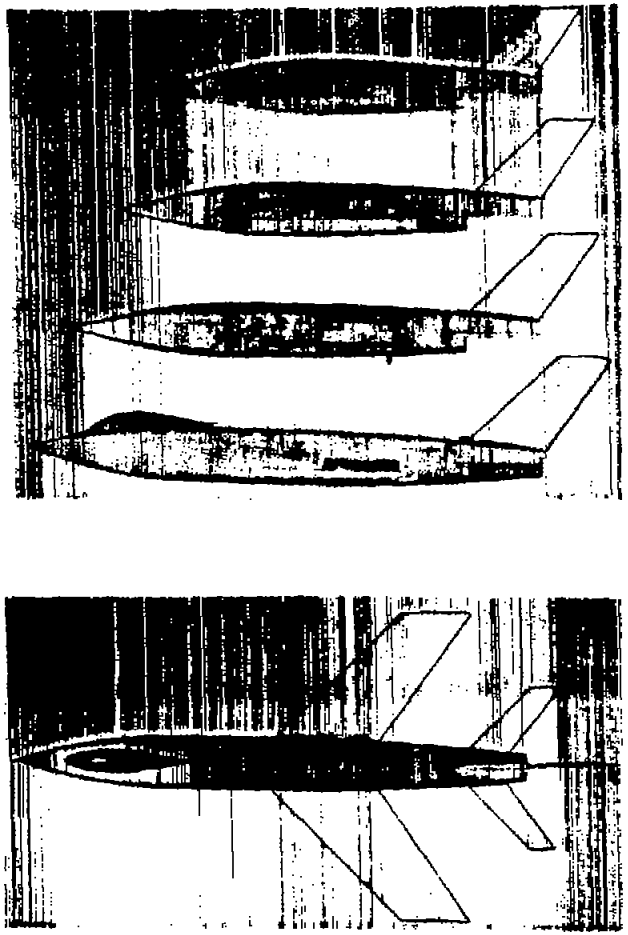

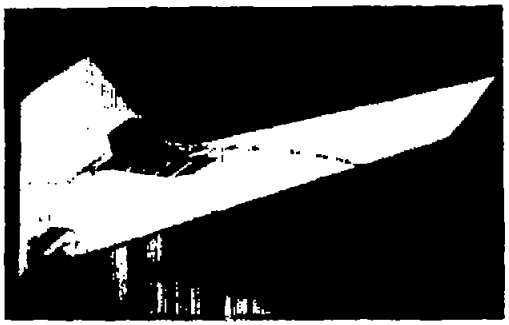

Wing alone mounted low with respect to moment center

Figure 3.- Photographs of models. L-57-147

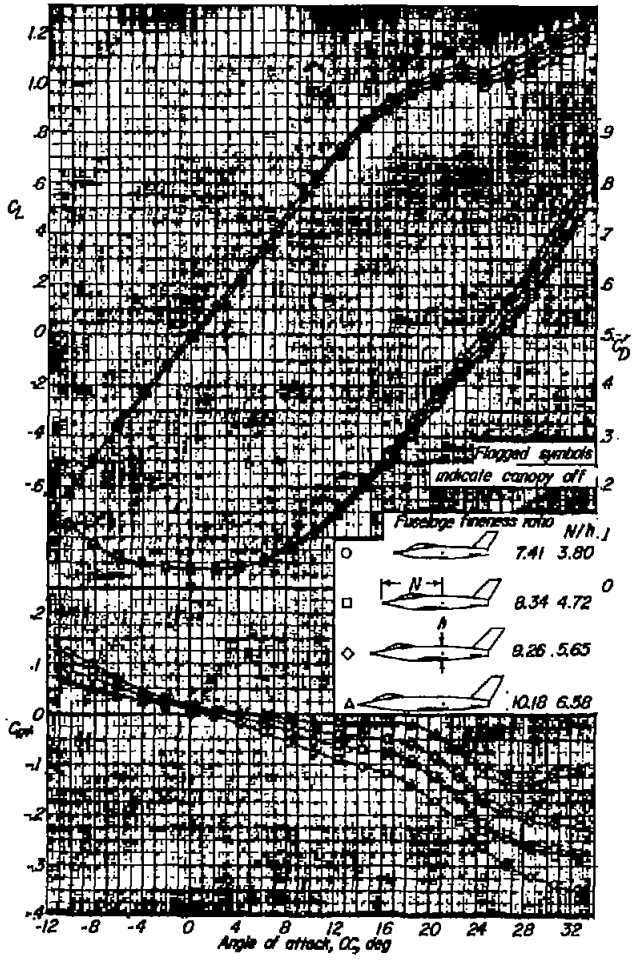

Figure 4.- Effect of fuselage nose length on the variation of C_L, C_D', and C_m with α for a complete 45° sweptback wing model having a fuselage with square cross sections. Canopy on and off; $\beta = 0°$.

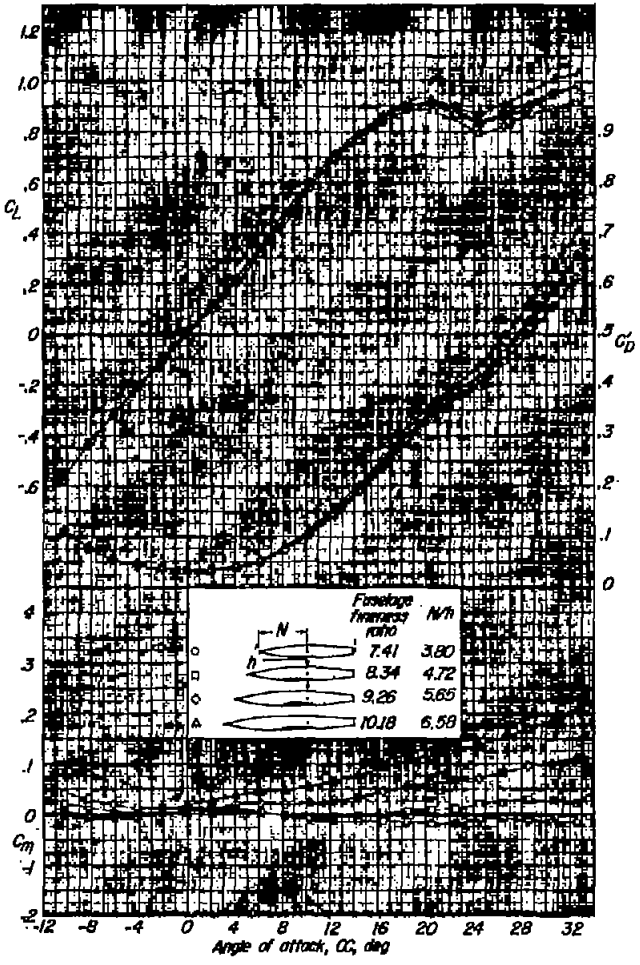

Figure 5.- Effect of fuselage nose length on the variation of C_L, C_D', and C_m with α for a wing-fuselage combination having a fuselage with square cross sections and a low wing of aspect ratio 3. Canopy off; $\beta = 0°$.

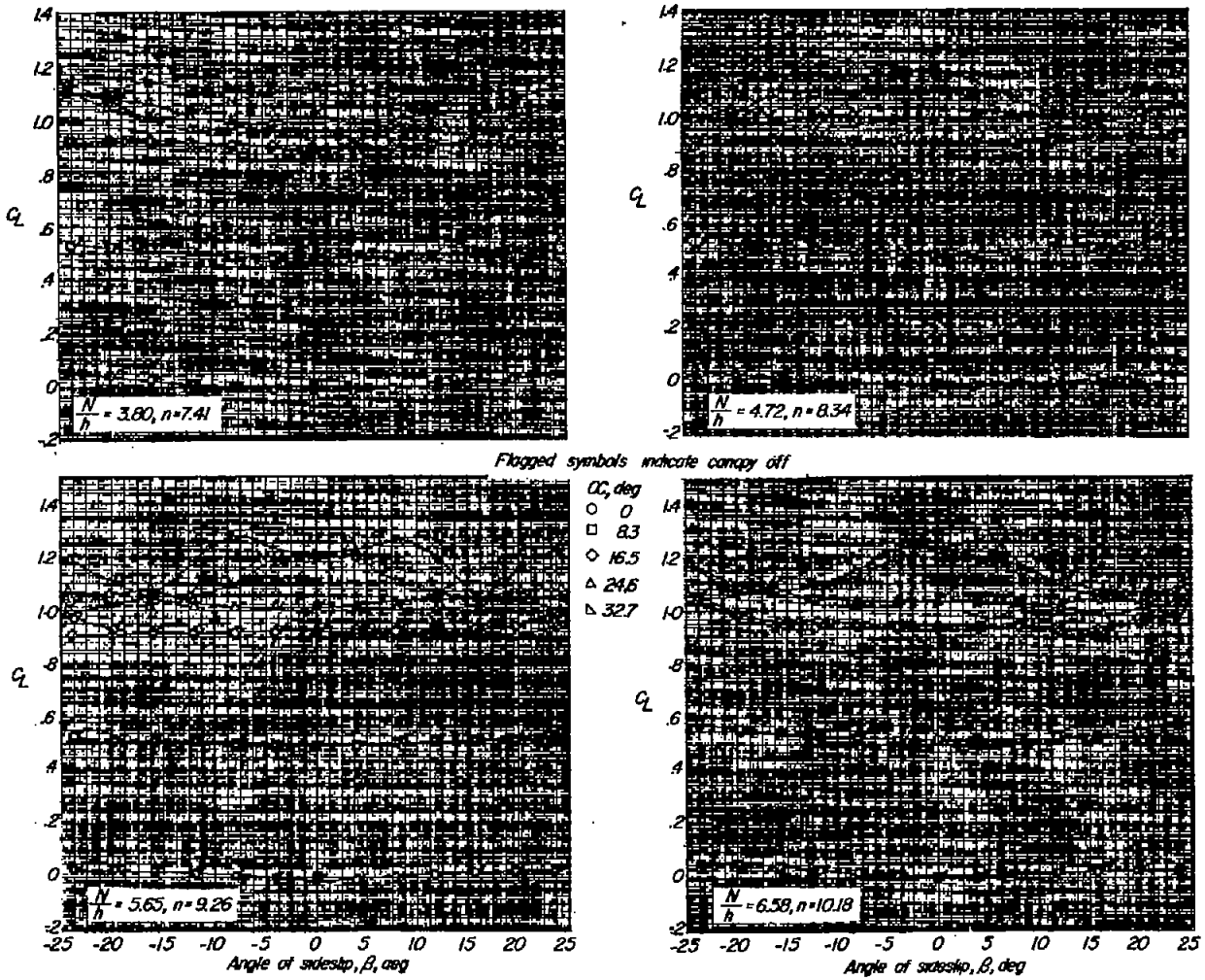

(a) Variation of C_L with β.

Figure 6.- Effect of canopy and fuselage nose length on variation of aerodynamic characteristics with angle of sideslip for a complete 45° sweptback wing model.

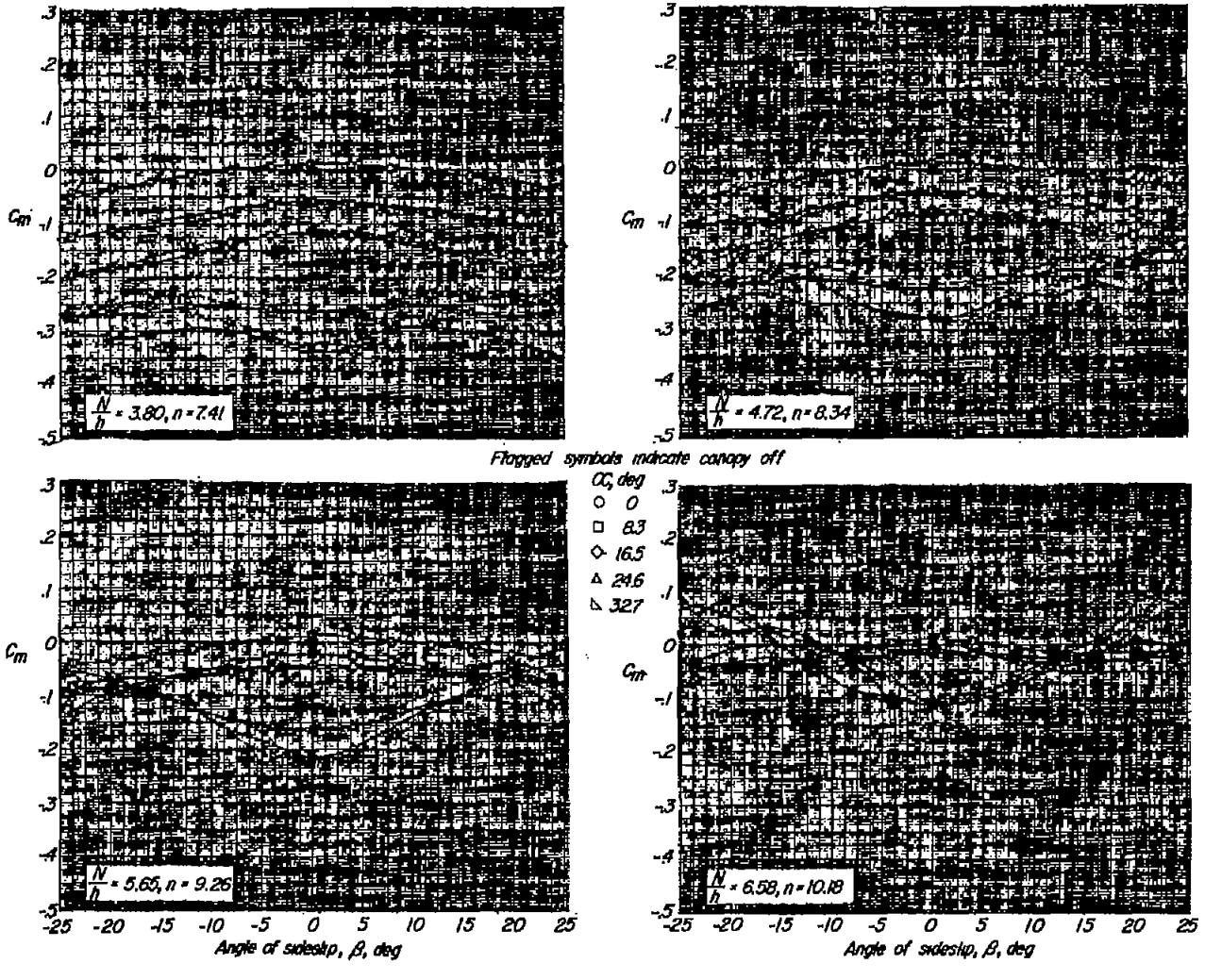

(b) Variation of C_m with β.

Figure 6.- Continued.

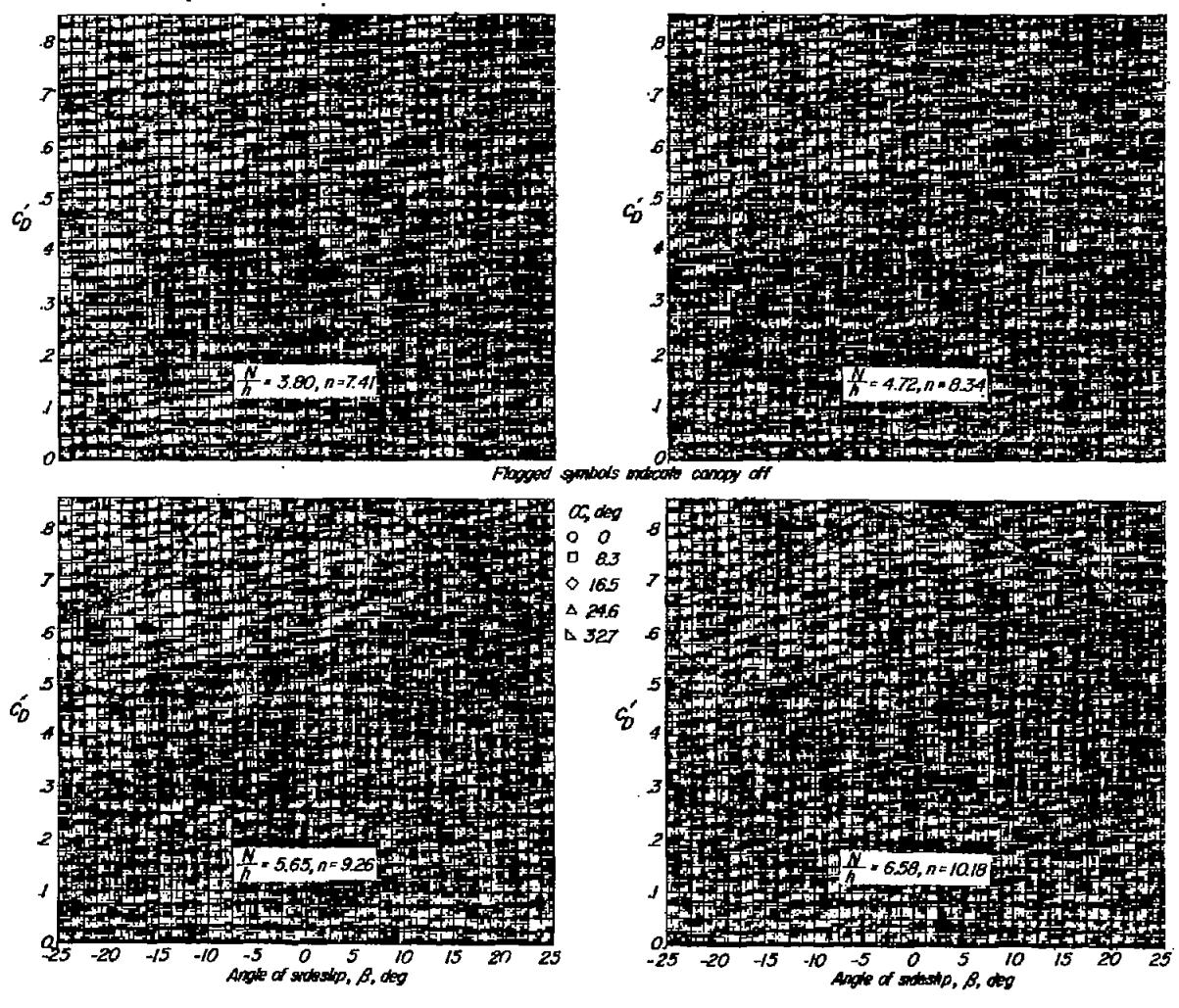

(c) Variation of C_D' with β.

Figure 6.- Continued.

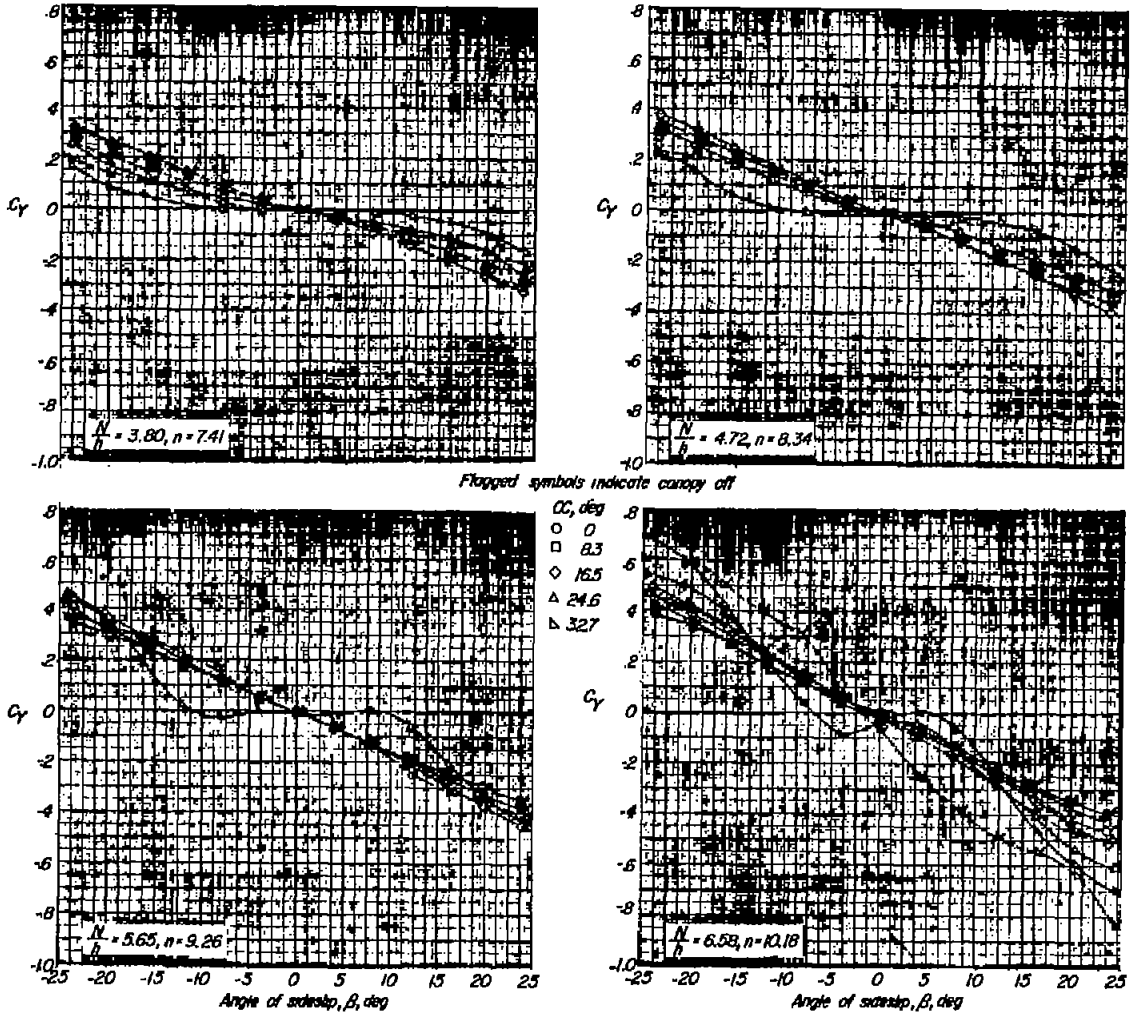

(d) Variation of C_Y with β.

Figure 6.- Continued.

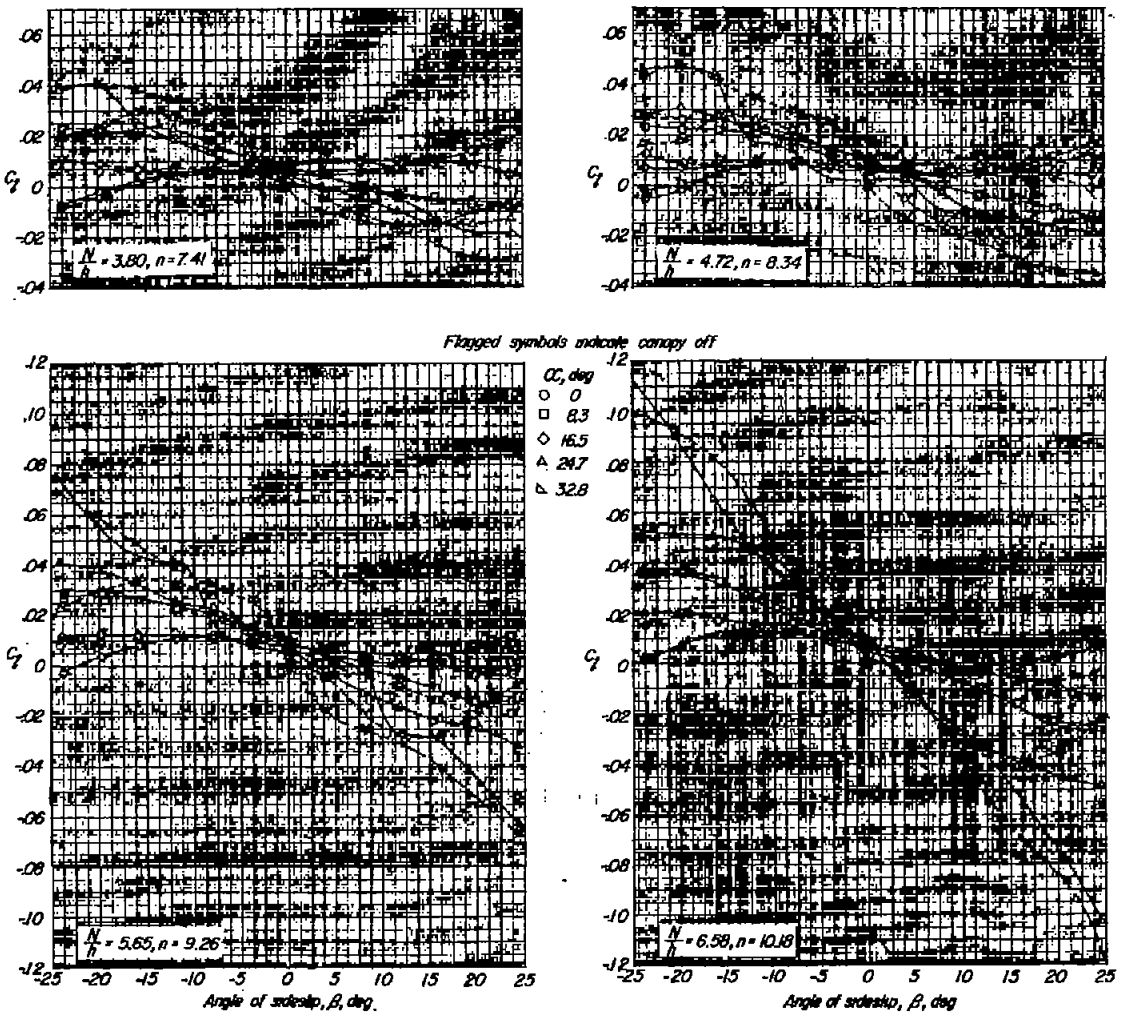

(e) Variation of C_l with β.

Figure 6.- Continued.

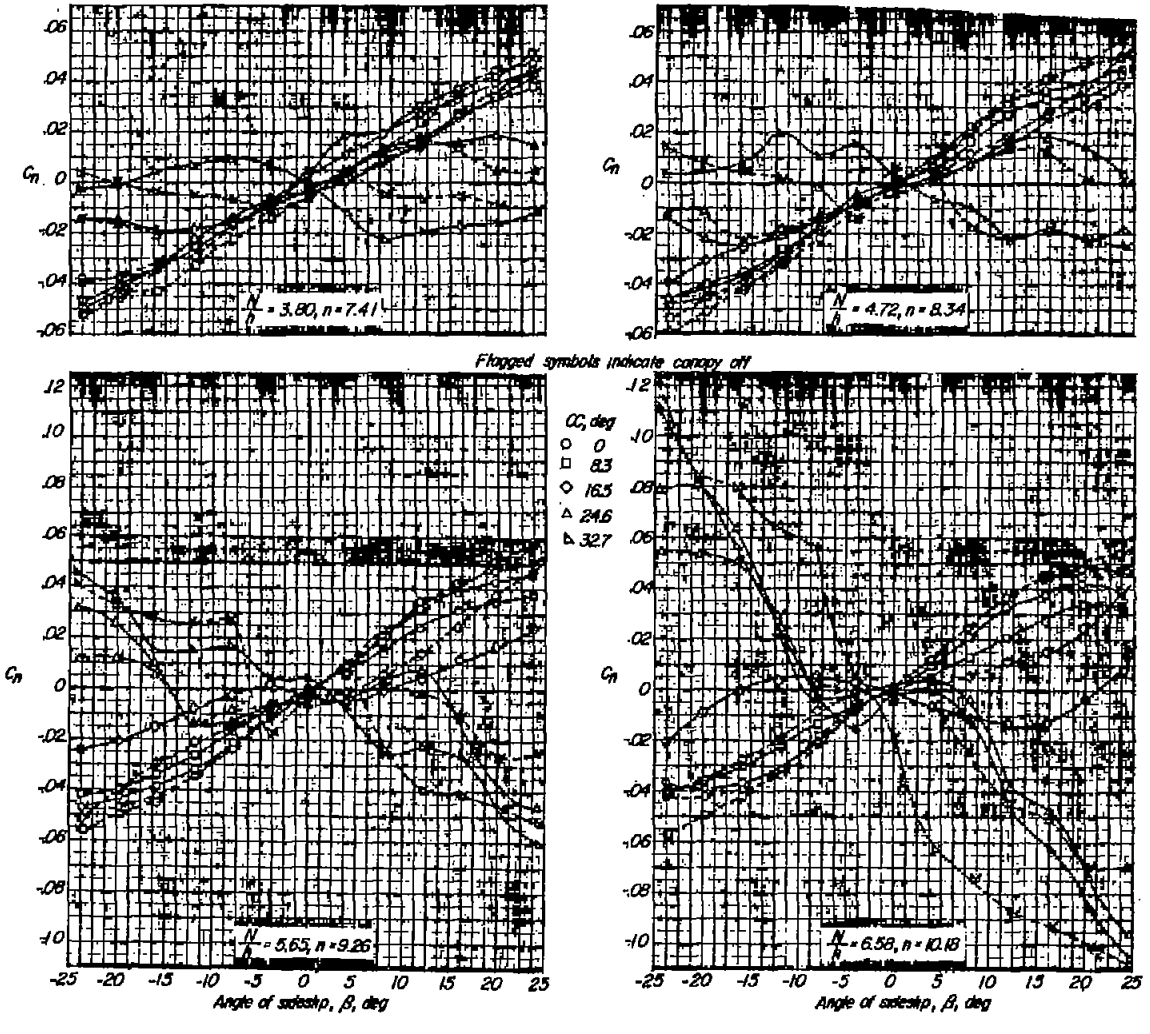

(f) Variation of C_n with β.

Figure 6.- Concluded.

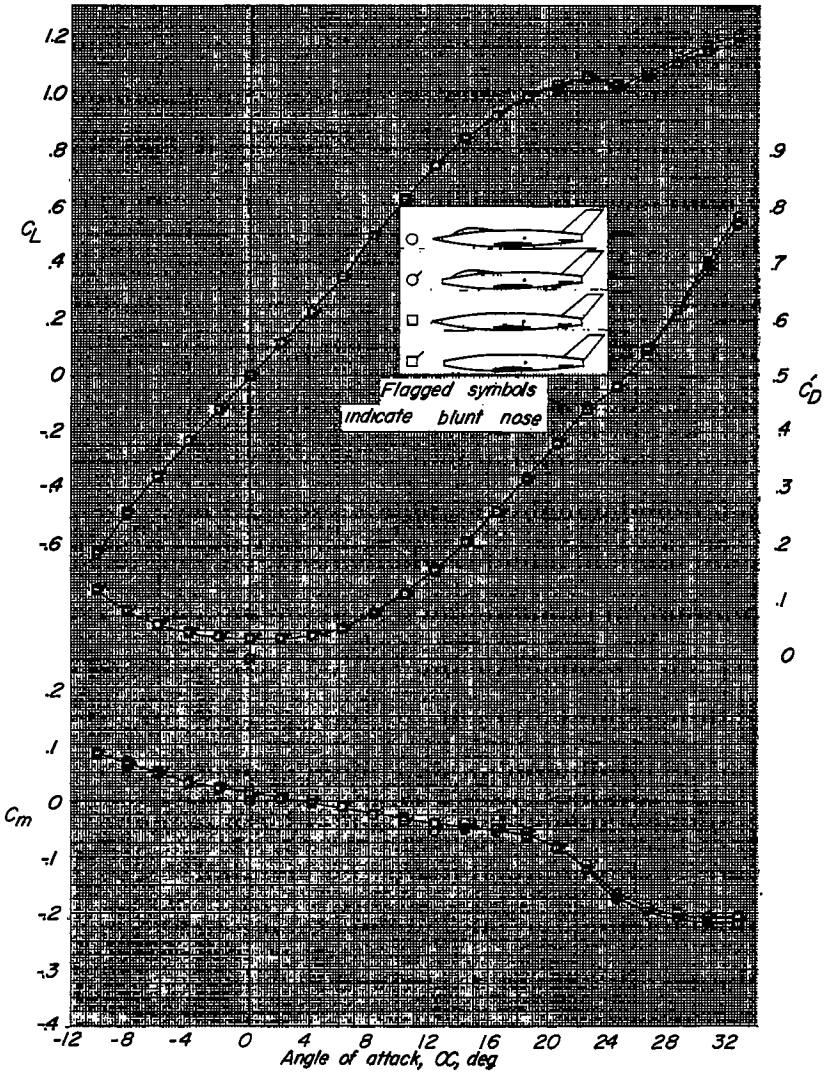

Figure 7.- Effect of blunting fuselage nose on variation of C_L, C_D', and C_m with α for a complete 45° sweptback wing model having a fuselage with square cross sections. Pointed fuselage of fineness ratio 9.26; blunt fuselage of fineness ratio 8.71; canopy on and off; $\beta = 0°$.

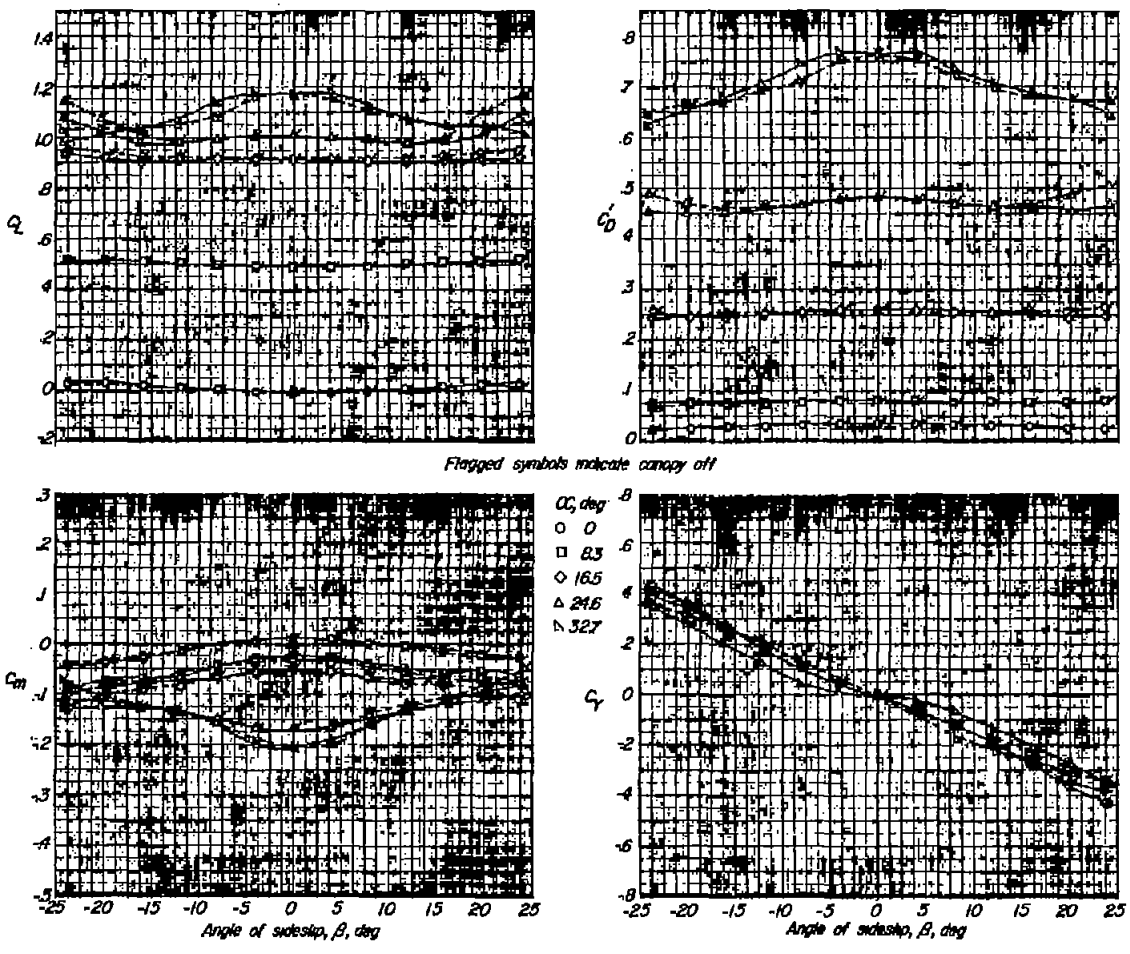

(a) Variation of C_L and C_m with β.

(b) Variation of C_D' and C_Y with β.

Figure 8.- Aerodynamic characteristics in sideslip of a complete 45° sweptback wing model having a blunt nose, a fineness ratio of 8.71, and a ratio of fuselage nose length to maximum depth of 5.09. Canopy on and off.

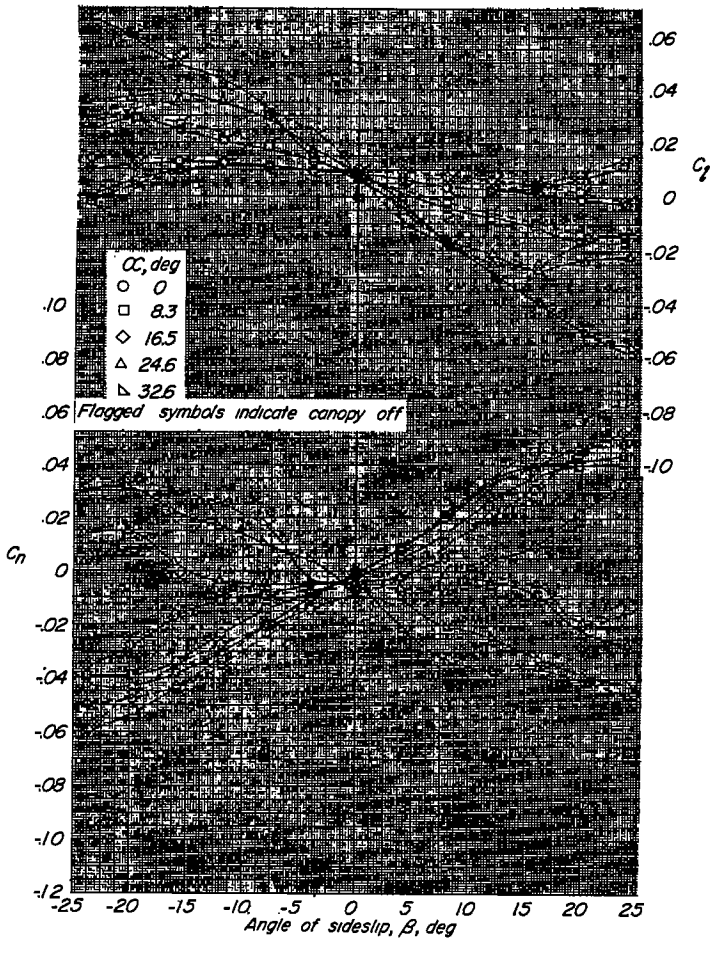

(c) Variation of C_l and C_n with β.

Figure 8.- Concluded.

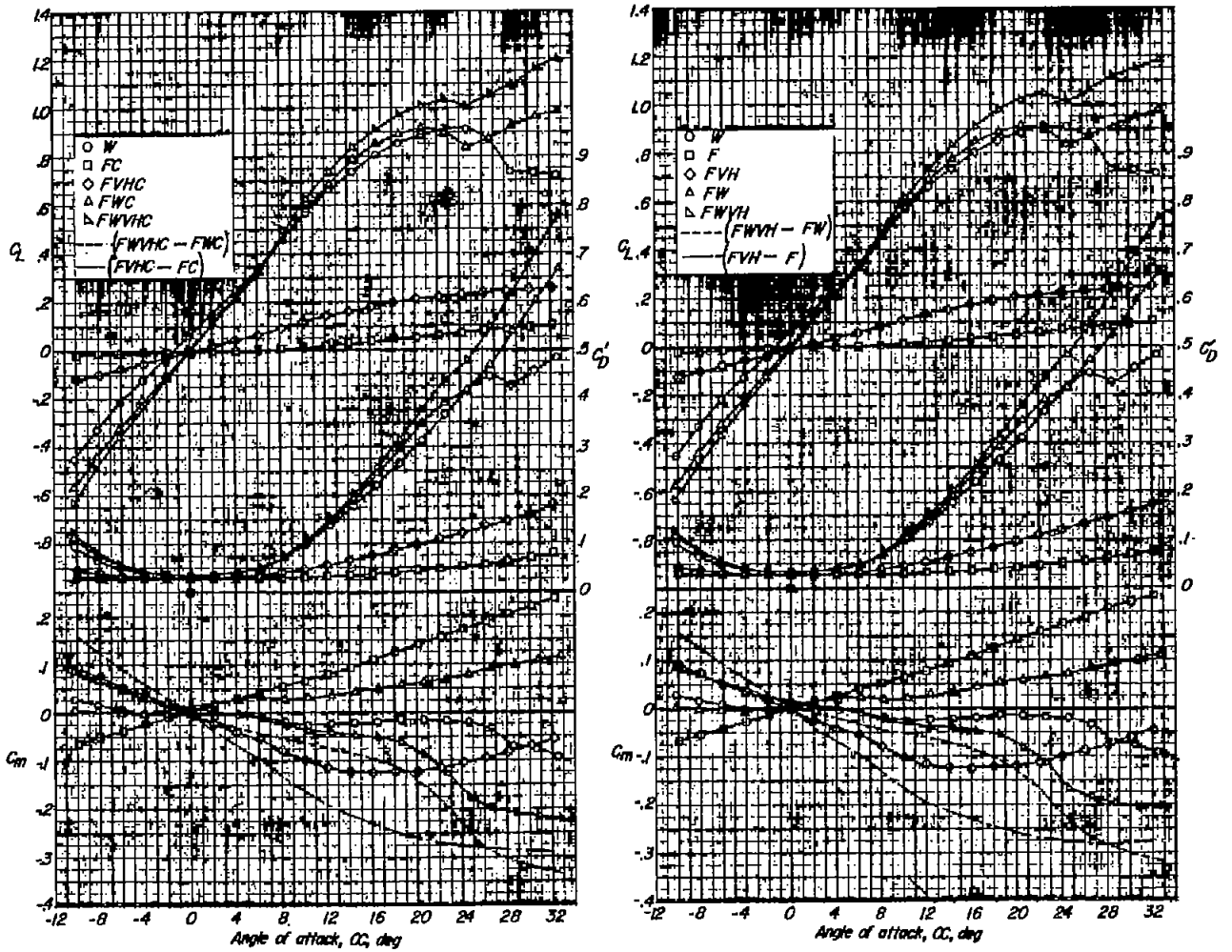

(a) Canopy on.

(b) Canopy off.

Figure 9.- Variation of C_L, C_D', and C_m with α for the components of a 45° sweptback wing model having a pointed fuselage of fineness ratio 9.26. $\beta = 0°$.

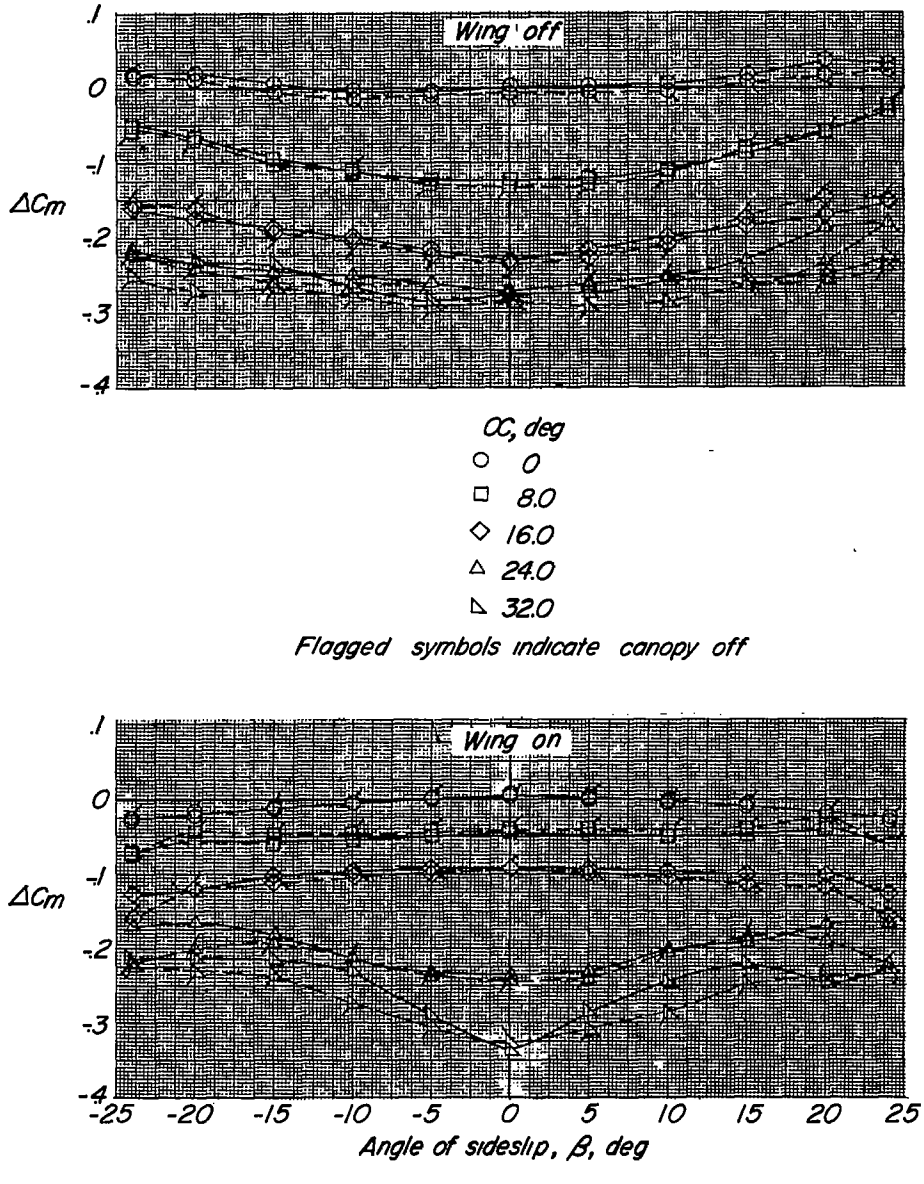

Figure 10.- Effect of canopy on the variation with angle of sideslip of the contribution of the tail assembly to the pitching-moment coefficient. Fuselage fineness ratio, 9.26; pointed nose; wing off and on.

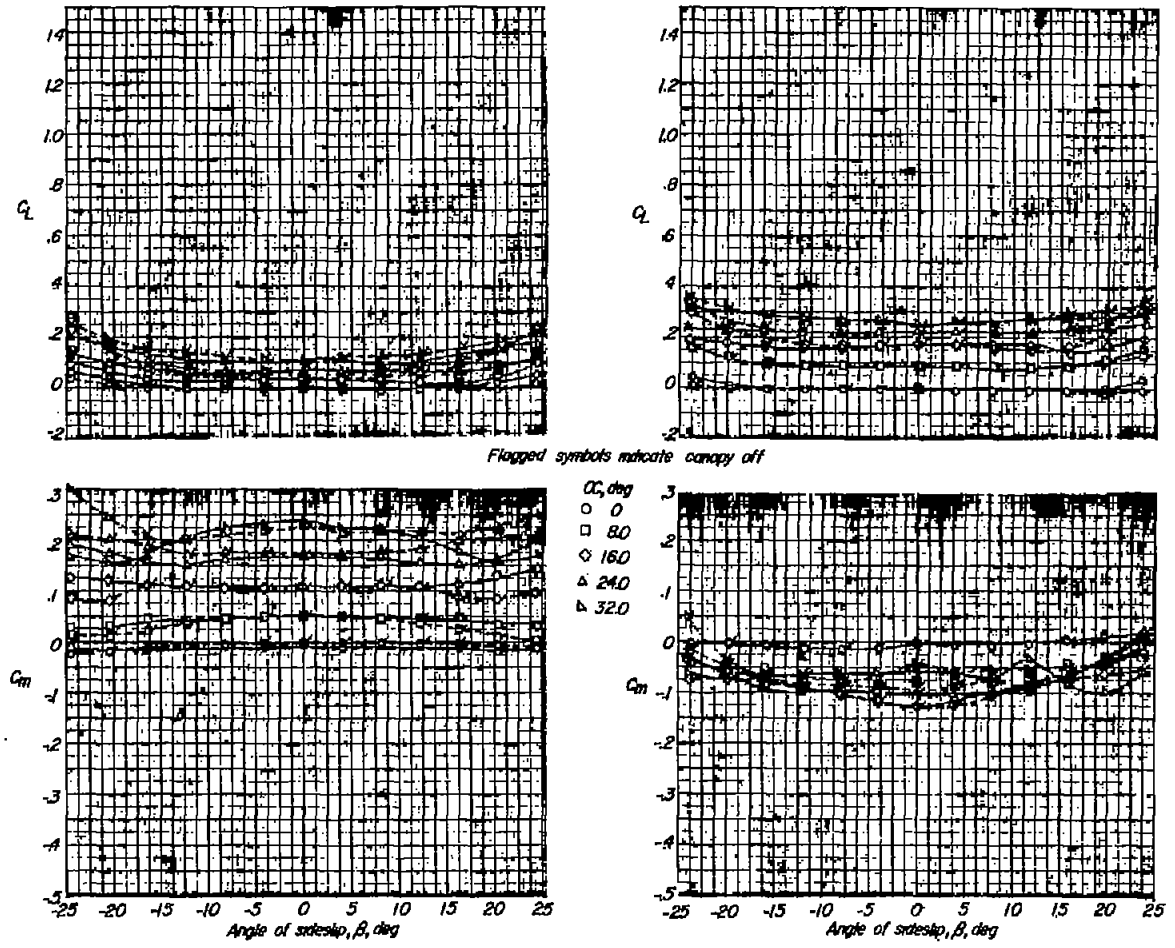

(a) Variation of C_L and C_m with β for F.

(b) Variation of C_L and C_m with β for FVH.

Figure 11.- Aerodynamic characteristics in sideslip of the components of a 45° sweptback wing model having a fuselage fineness ratio of 9.26 and a ratio of fuselage nose length to maximum depth of 5.65. Pointed nose; canopy on and off; wing off.

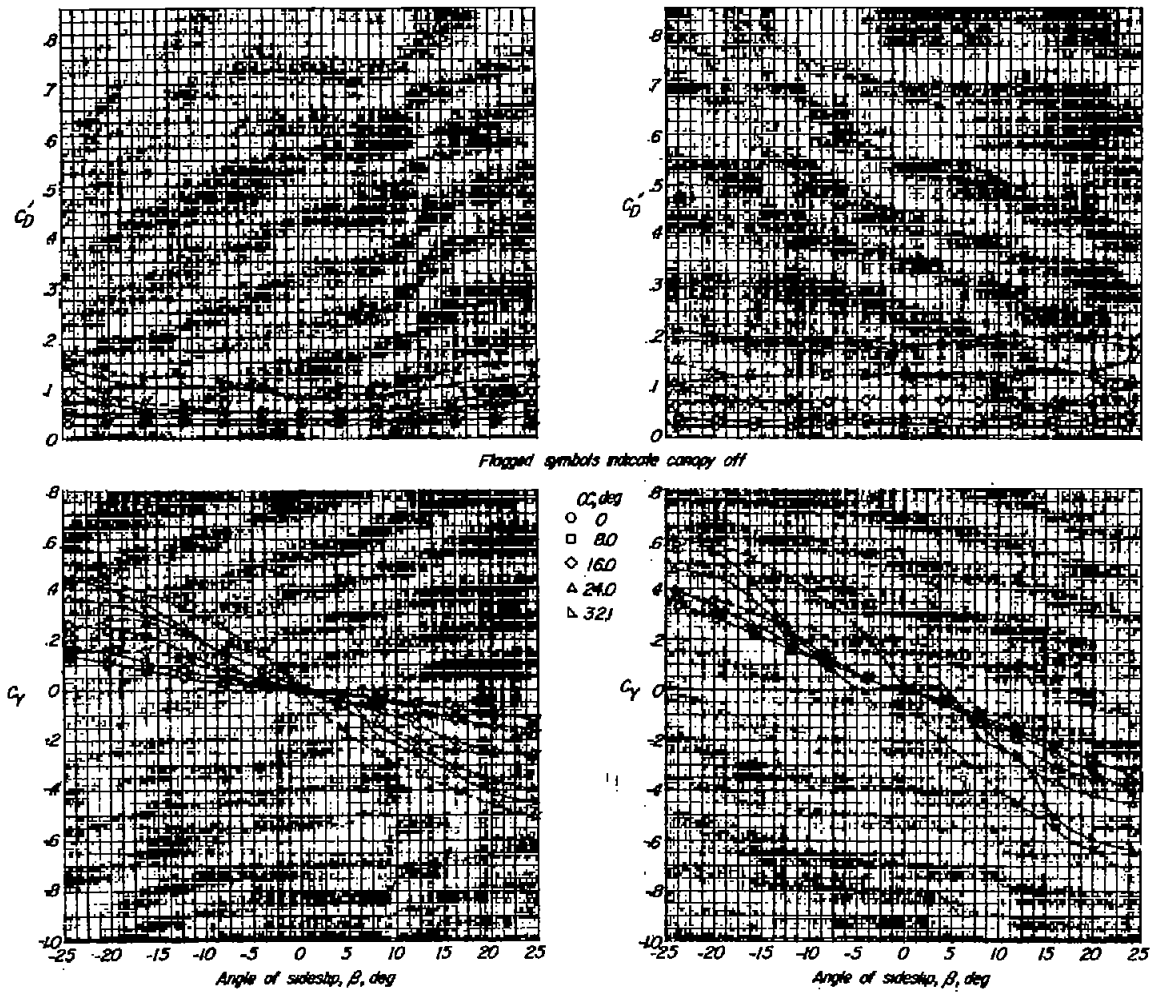

(c) Variation of C_D' and C_Y with β for F.

(d) Variation of C_D' and C_Y with β for FVH.

Figure 11.- Continued.

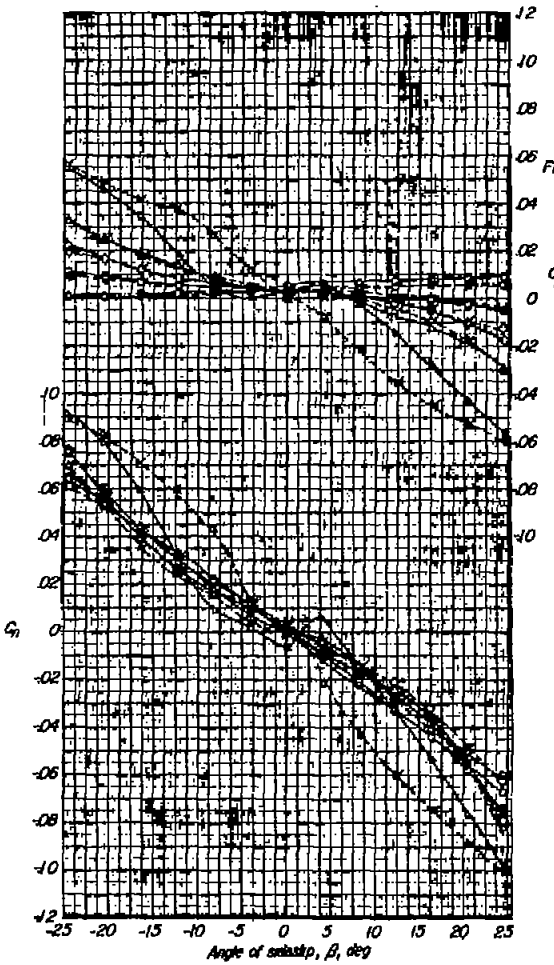

(e) Variation of C_l and C_n with β for F.

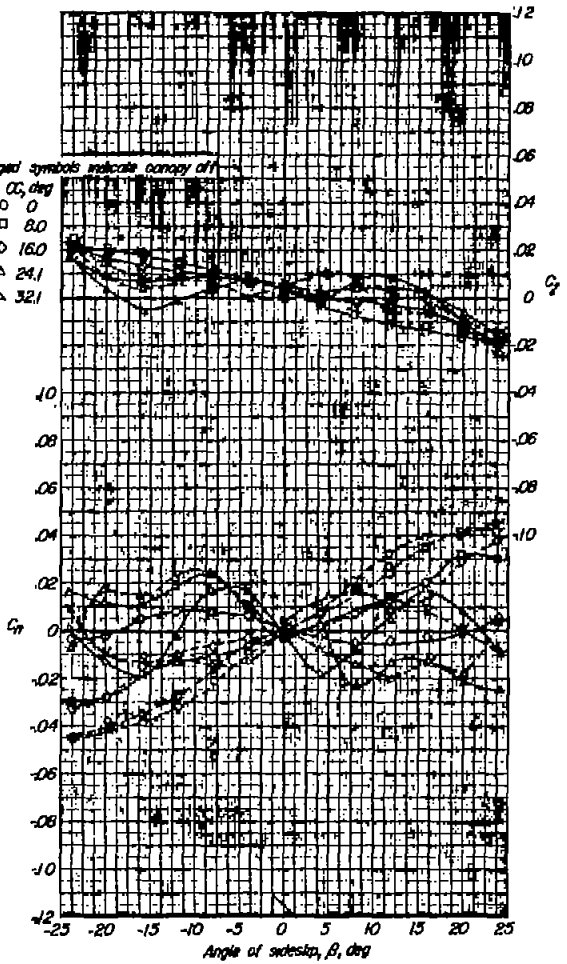

(f) Variation of C_l and C_n with β for FVH.

Figure 11.- Concluded.

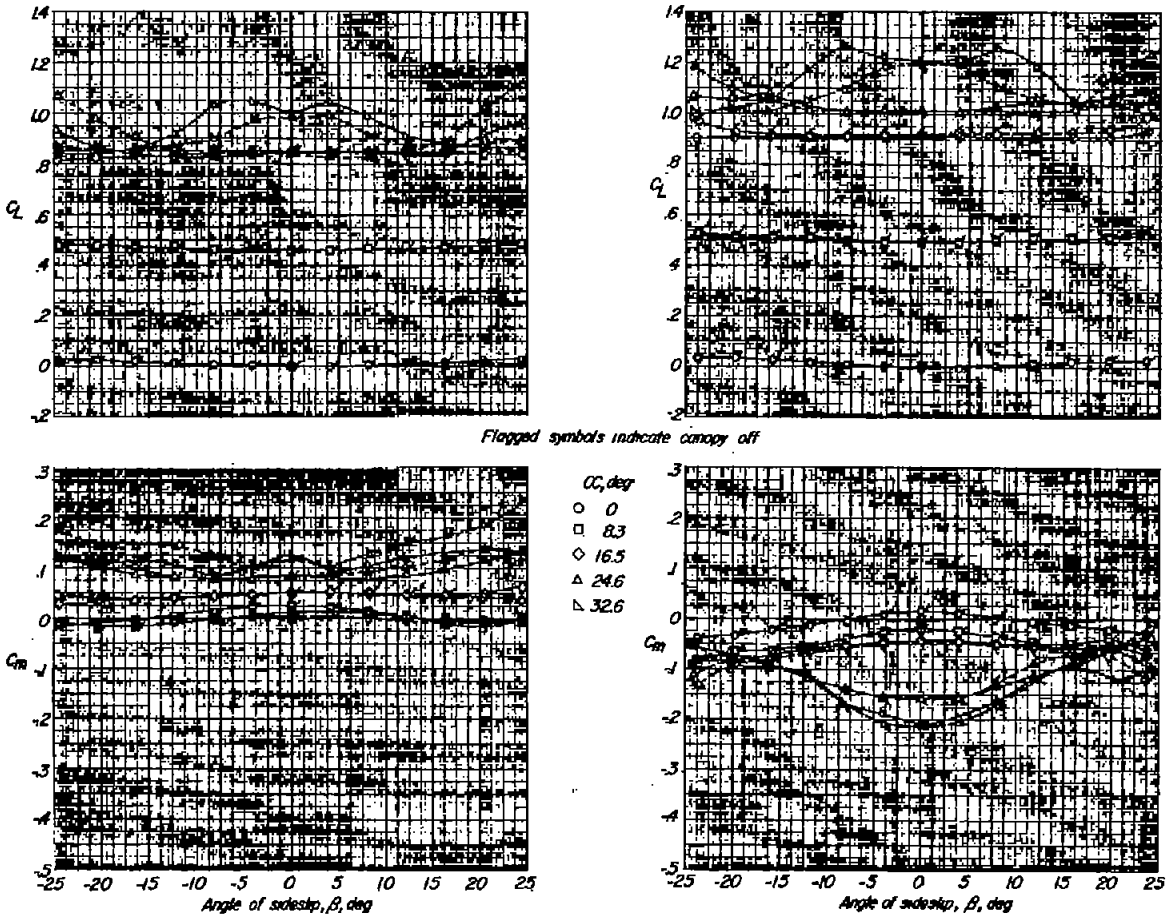

(a) Variation of C_L and C_m with β for FW.

(b) Variation of C_L and C_m with β for FWVH.

Figure 12.- Aerodynamic characteristics in sideslip of the components of a 45° sweptback wing model having a fuselage fineness ratio of 9.26 and a ratio of fuselage nose length to maximum depth of 5.65. Pointed fuselage; canopy on and off; wing on.

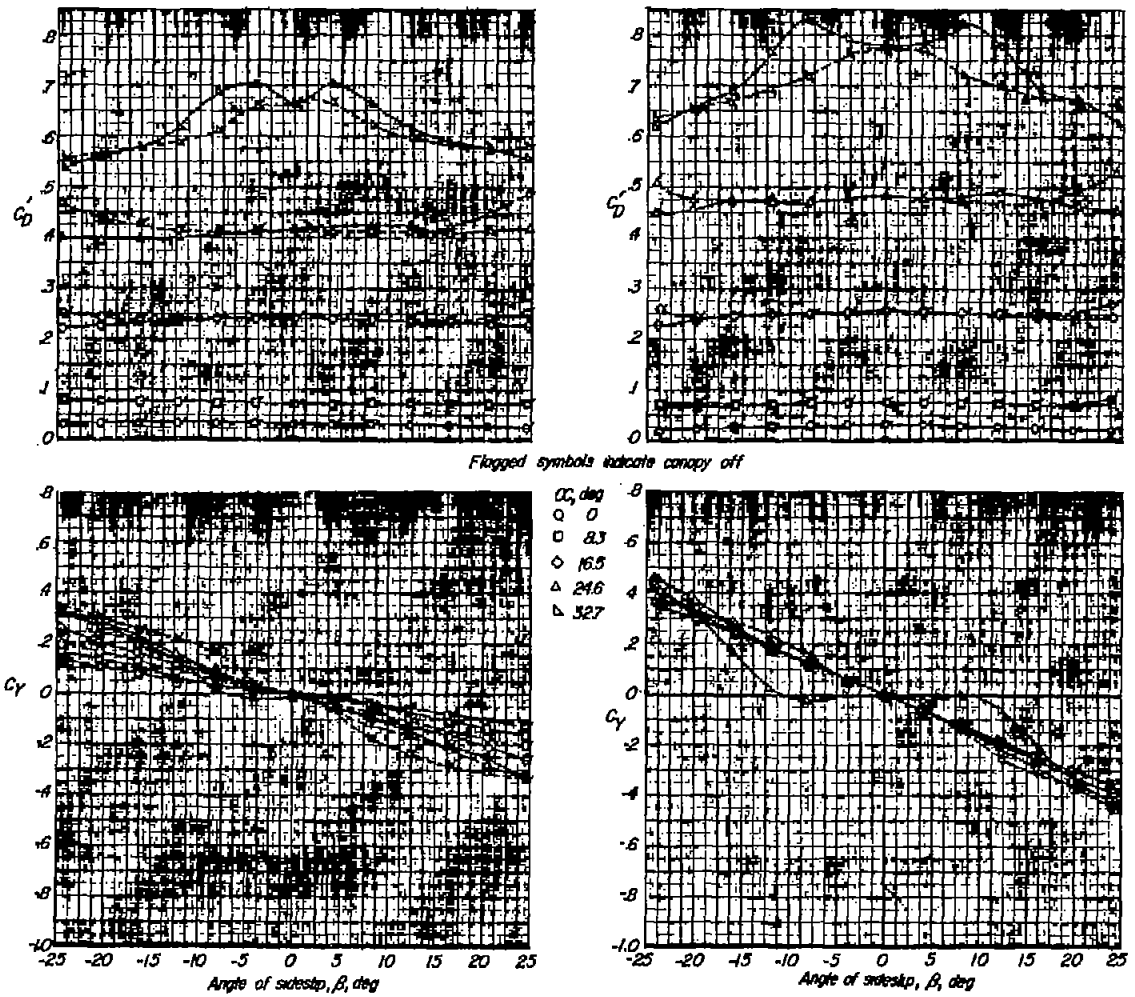

(c) Variation of C_D' and C_Y with β for FW.

(d) Variation of C_D' and C_Y with β for FWVH.

Figure 12.- Continued.

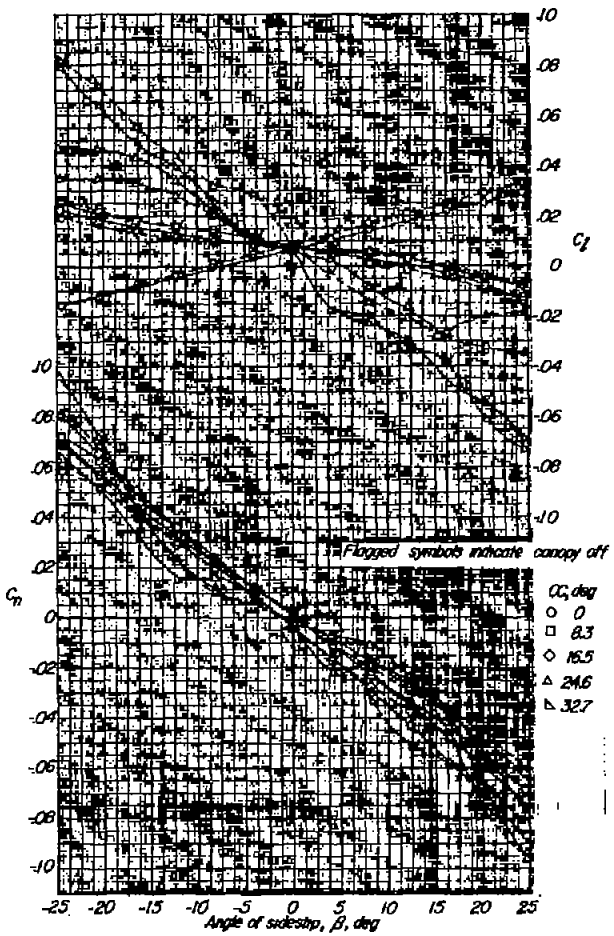

(e) Variation of C_l and C_n with β for FW.

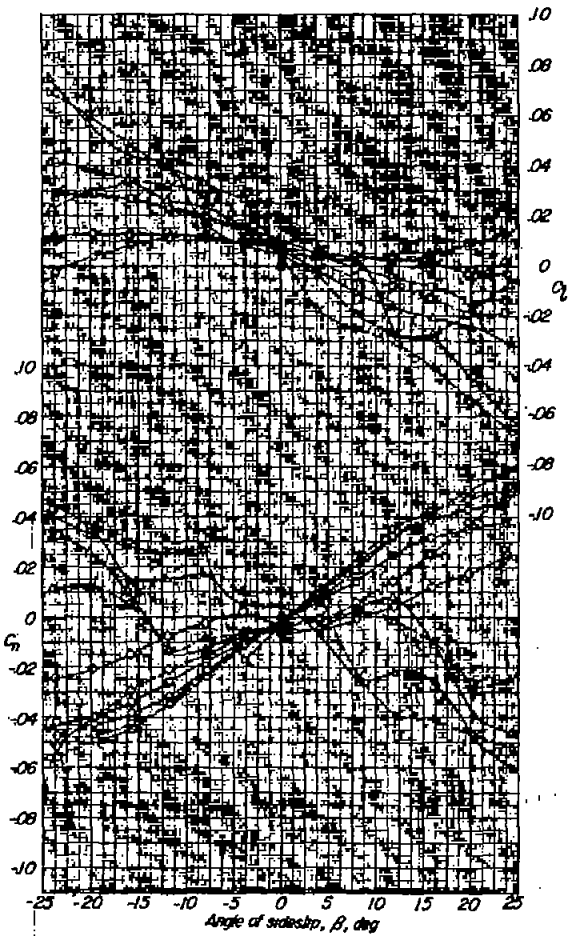

(f) Variation of C_l and C_n with β for FWVH.

Figure 12.- Concluded.

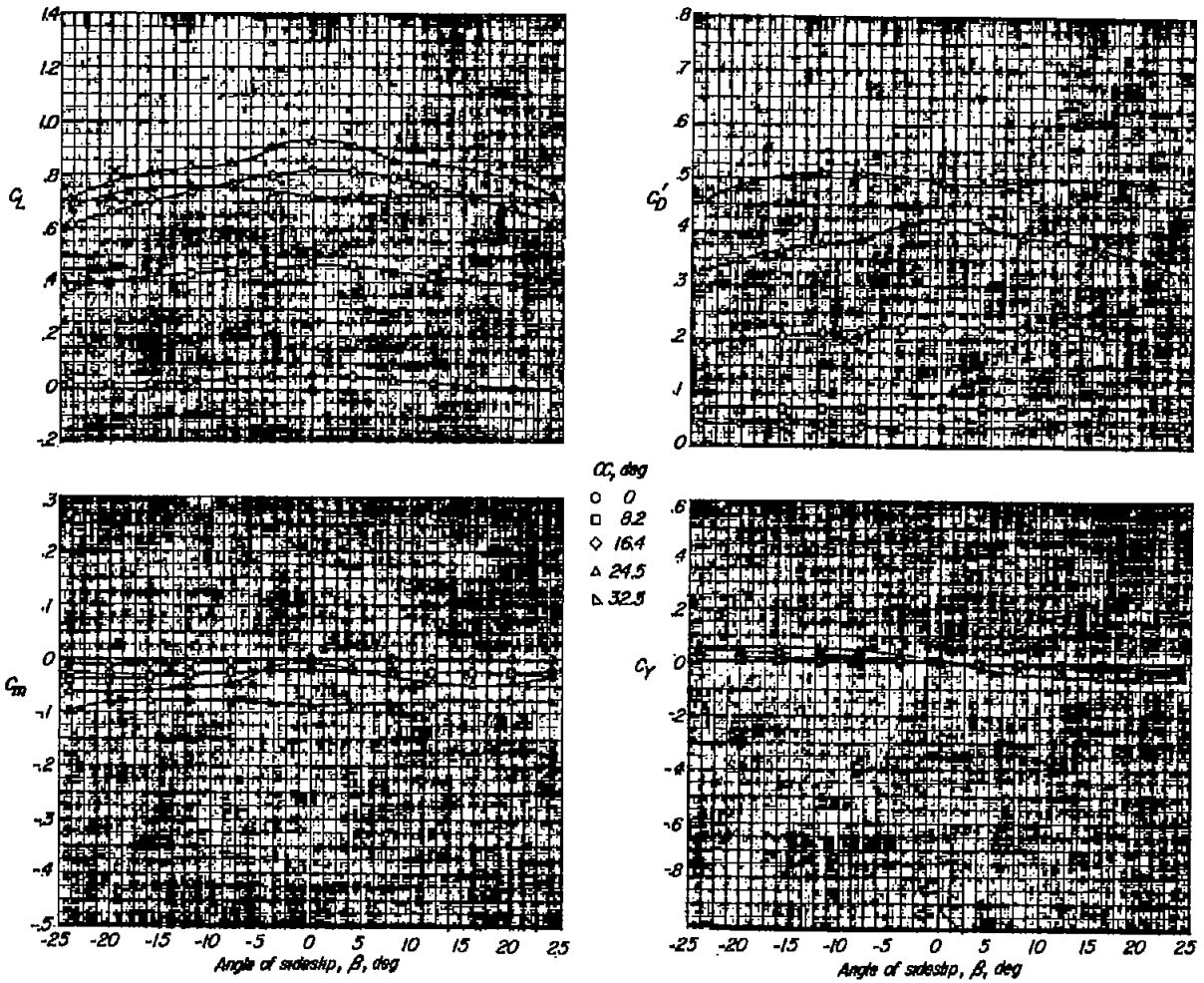

(a) Variation of C_L and C_m with β.

(b) Variation of C_D' and C_Y with β.

Figure 13.- Aerodynamic characteristics in sideslip of a 45° sweptback wing having an aspect ratio of 3 and mounted in low position with respect to moment center of model.

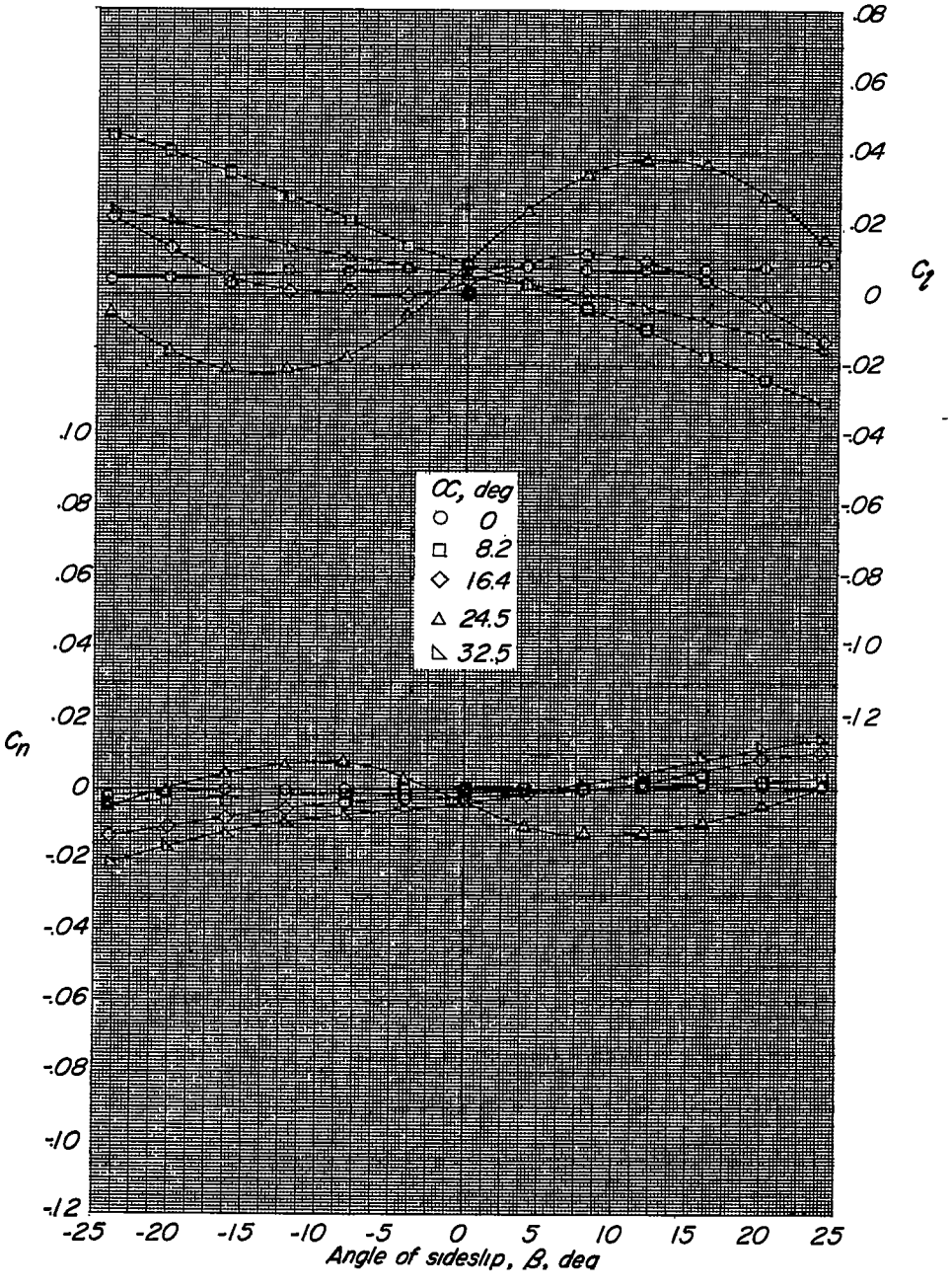

(c) Variation of C_l and C_n with β.

Figure 13.- Concluded.

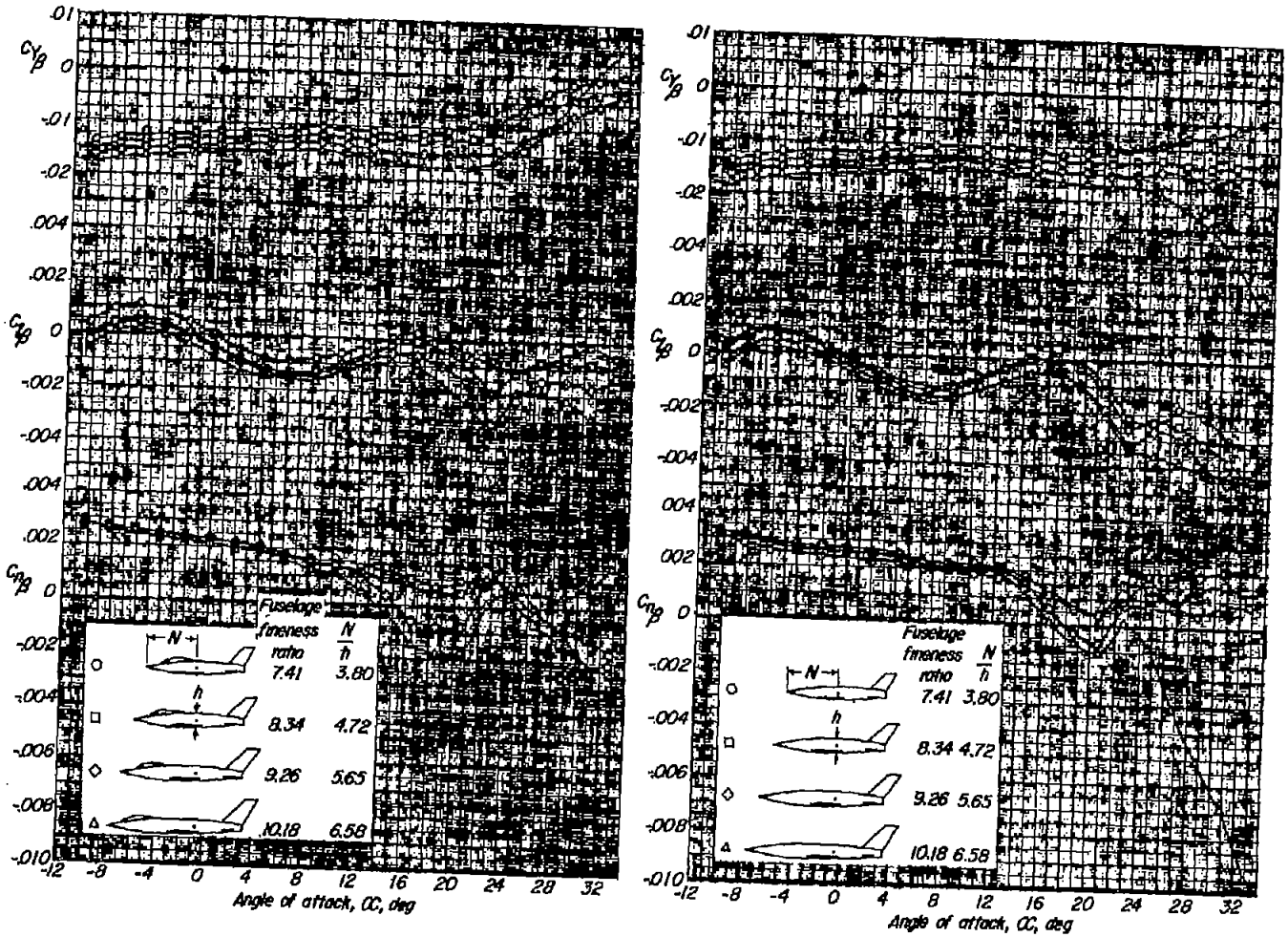

(a) Canopy on.

(b) Canopy off.

Figure 14.- Effect of fuselage nose length on the variation of C_{Y_β}, C_{l_β}, and C_{n_β} for a complete 45° sweptback wing model having a fuselage with square cross sections. Pointed nose.

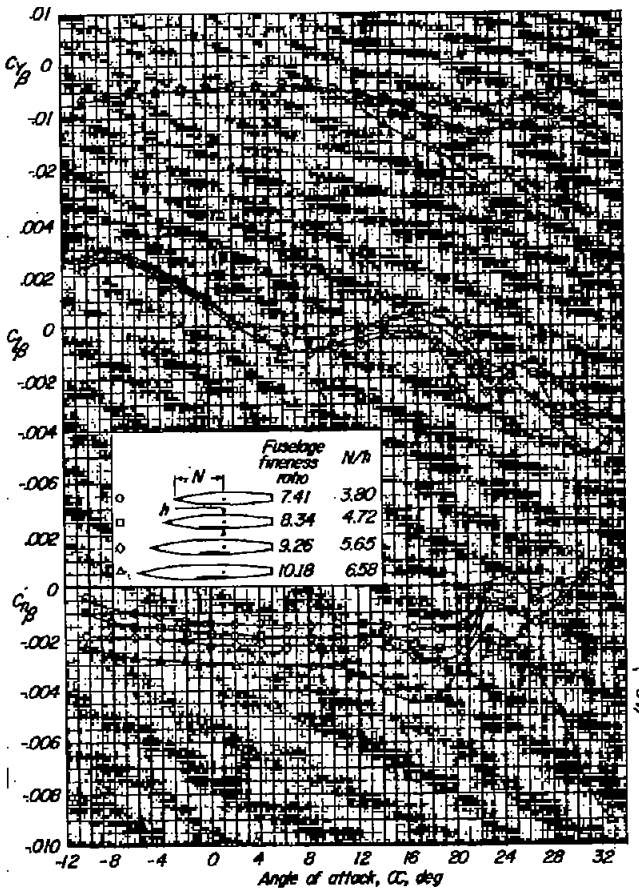

Figure 15.- Effect of fuselage nose length on the variation of C_{Y_β}, C_{l_β}, and C_{n_β} with α for a wing-fuselage combination having a fuselage with square cross sections and a low wing of aspect ratio 3. Canopy off.

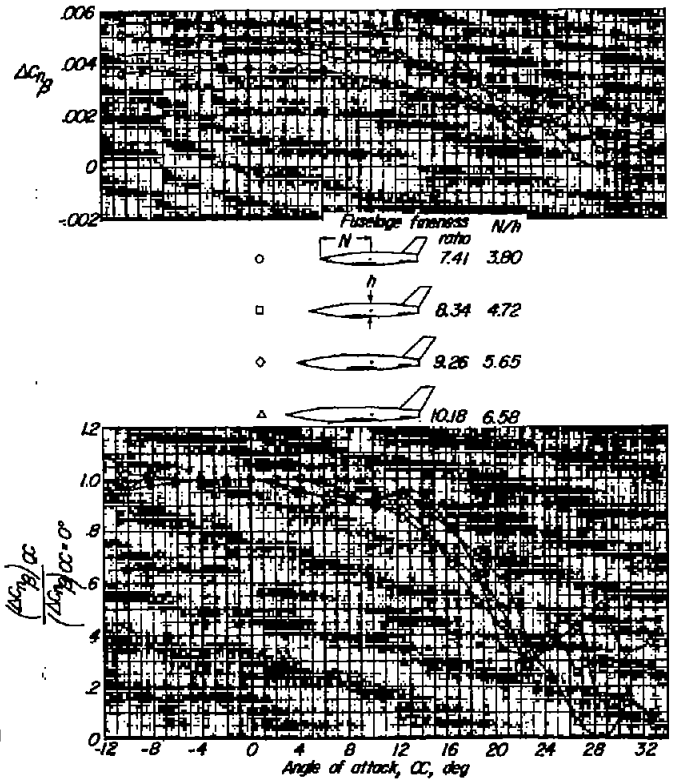

Figure 16.- Effect of fuselage nose length on contribution of tail assembly to C_{n_β} for a model having a fuselage with square sections. (Vertical-tail size varies with fuselage nose length.)

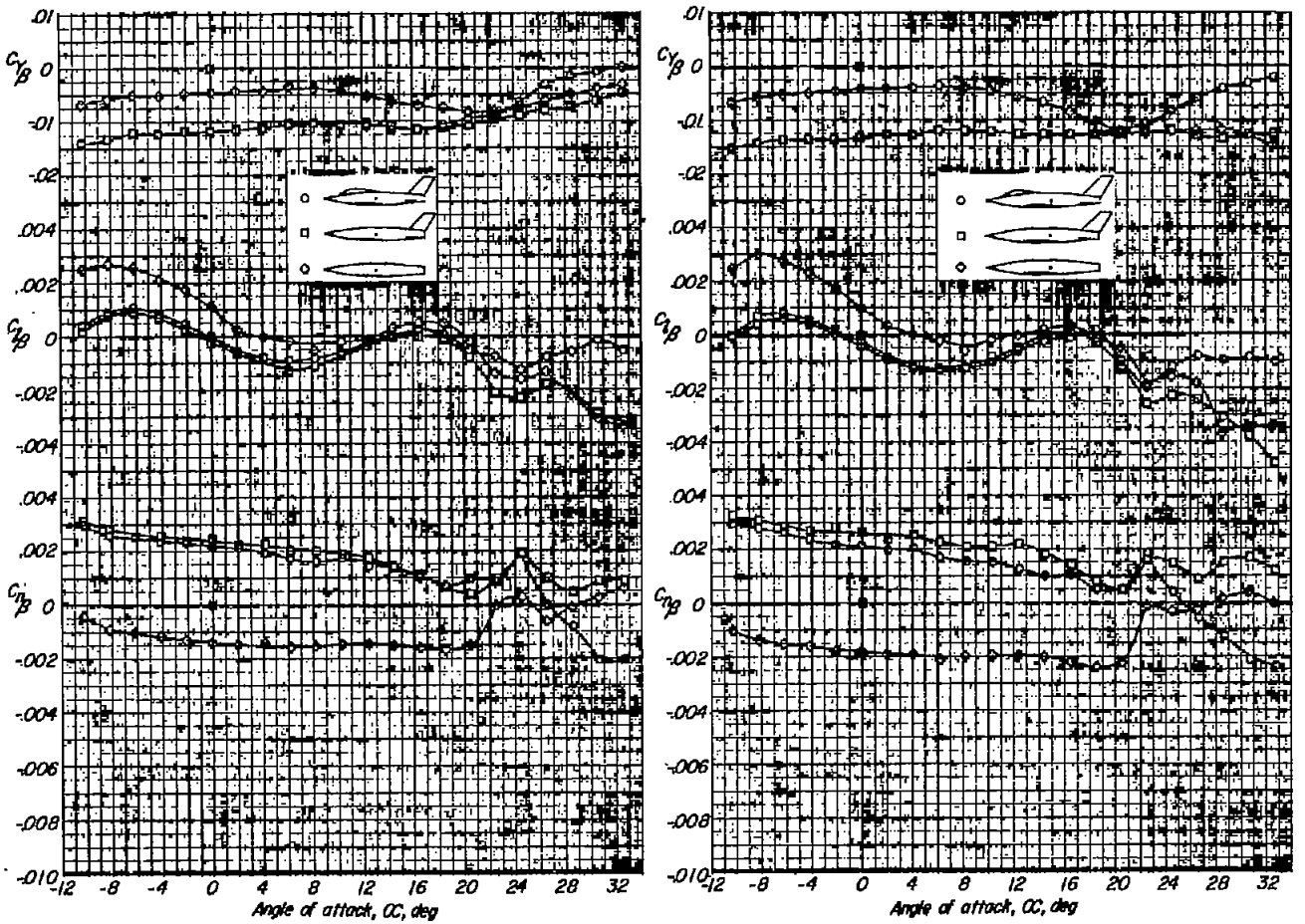

(a) Fuselage of fineness ratio 7.41 (pointed nose).

(b) Fuselage of fineness ratio 8.34 (pointed nose).

Figure 17.- Effect of canopy on the variation of C_{Y_β}, C_{l_β}, and C_{n_β} for a 45° sweptback wing model having a fuselage with square cross sections.

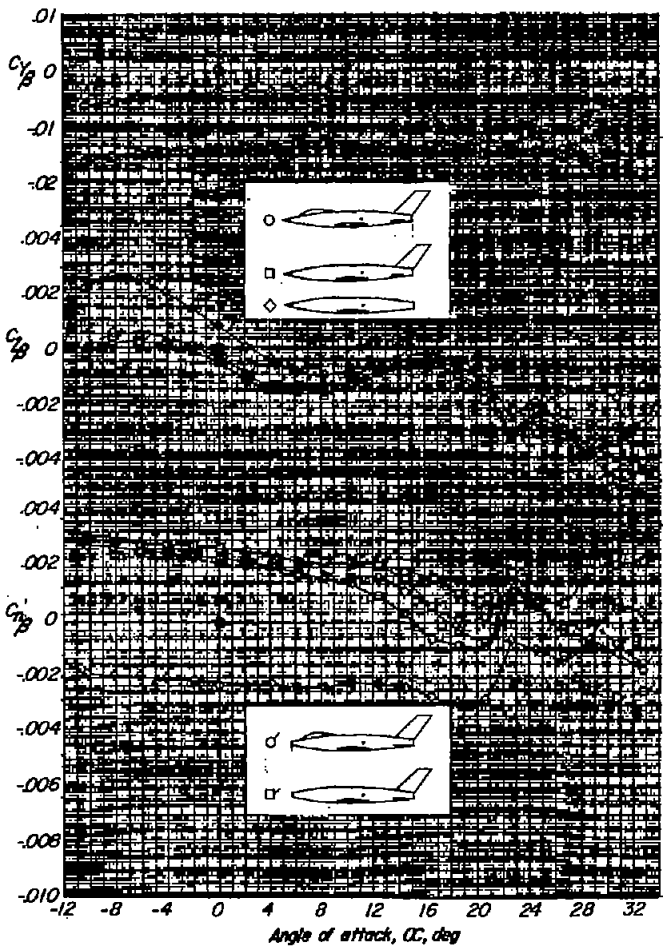

(c) Fuselages of fineness ratio 9.26 (pointed nose) and 8.71 (blunt nose).

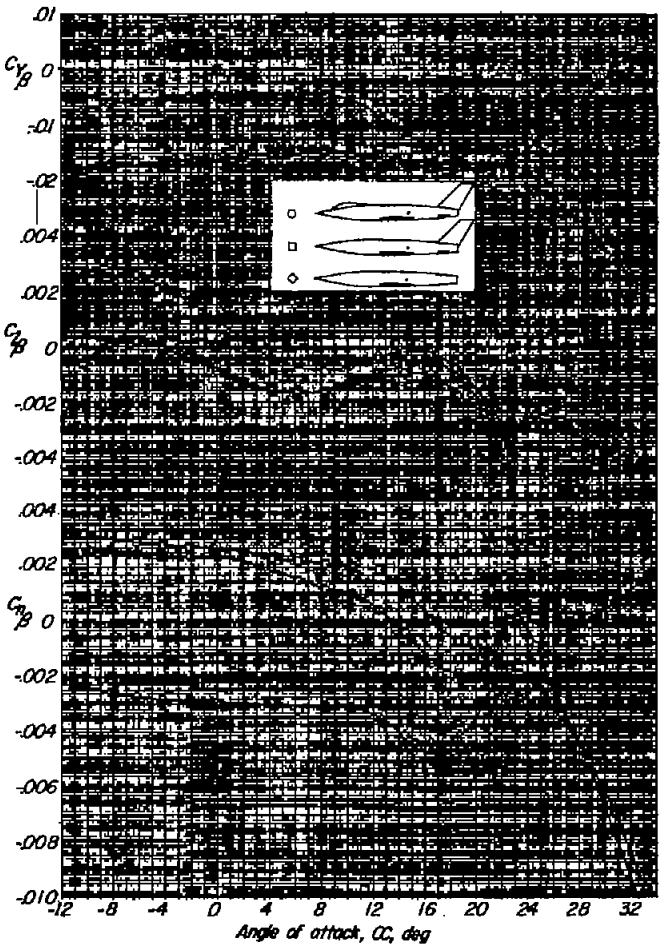

(d) Fuselage of fineness ratio 10.18.

Figure 17.- Concluded.

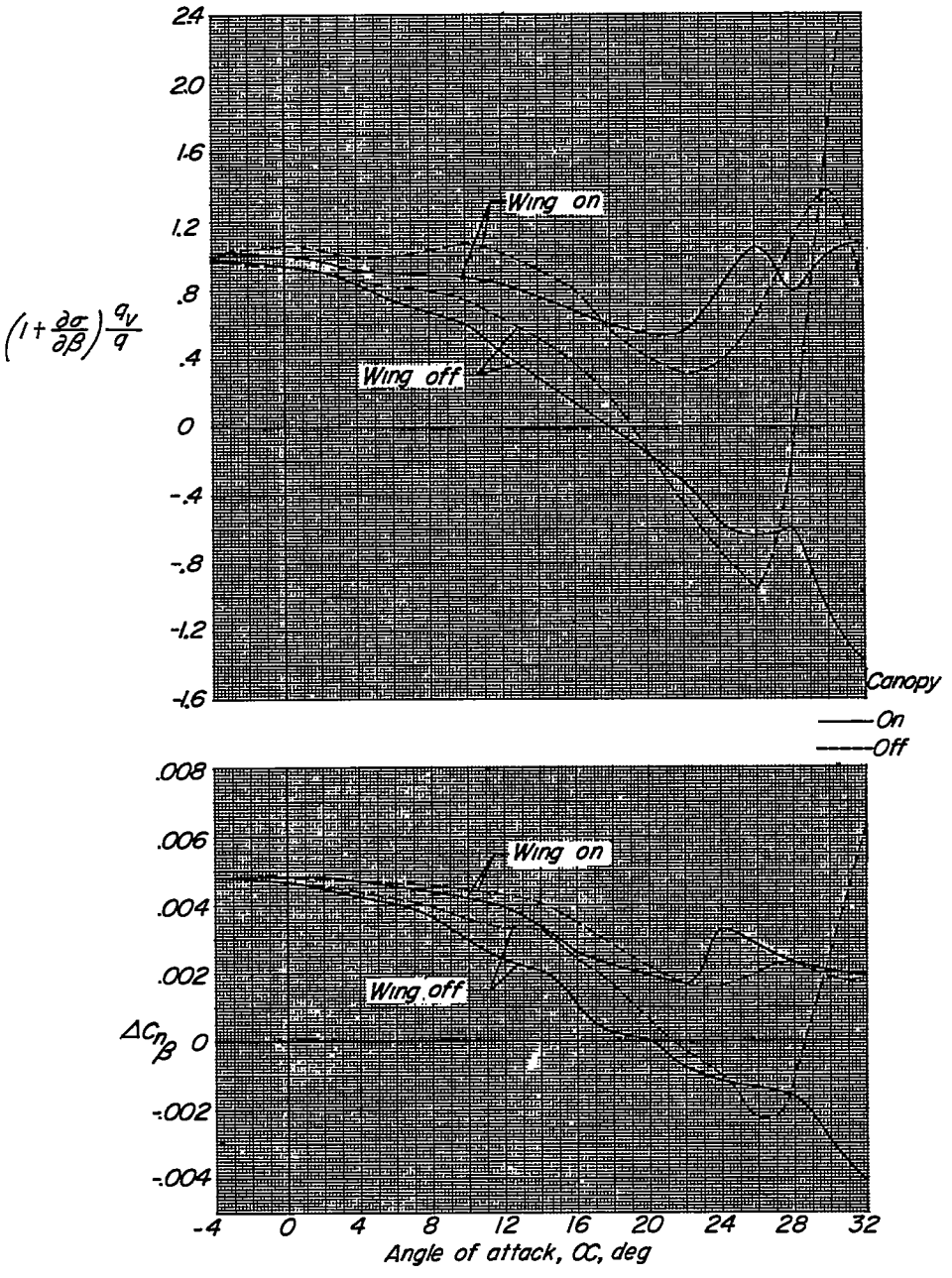

Figure 18.- Effect of canopy and wing on variation of $\left(1+\frac{\partial\sigma}{\partial\beta}\right)\frac{q_v}{q}$ and ΔC_{n_β} for a 45° sweptback wing model having a pointed fuselage of fineness ratio 9.26.

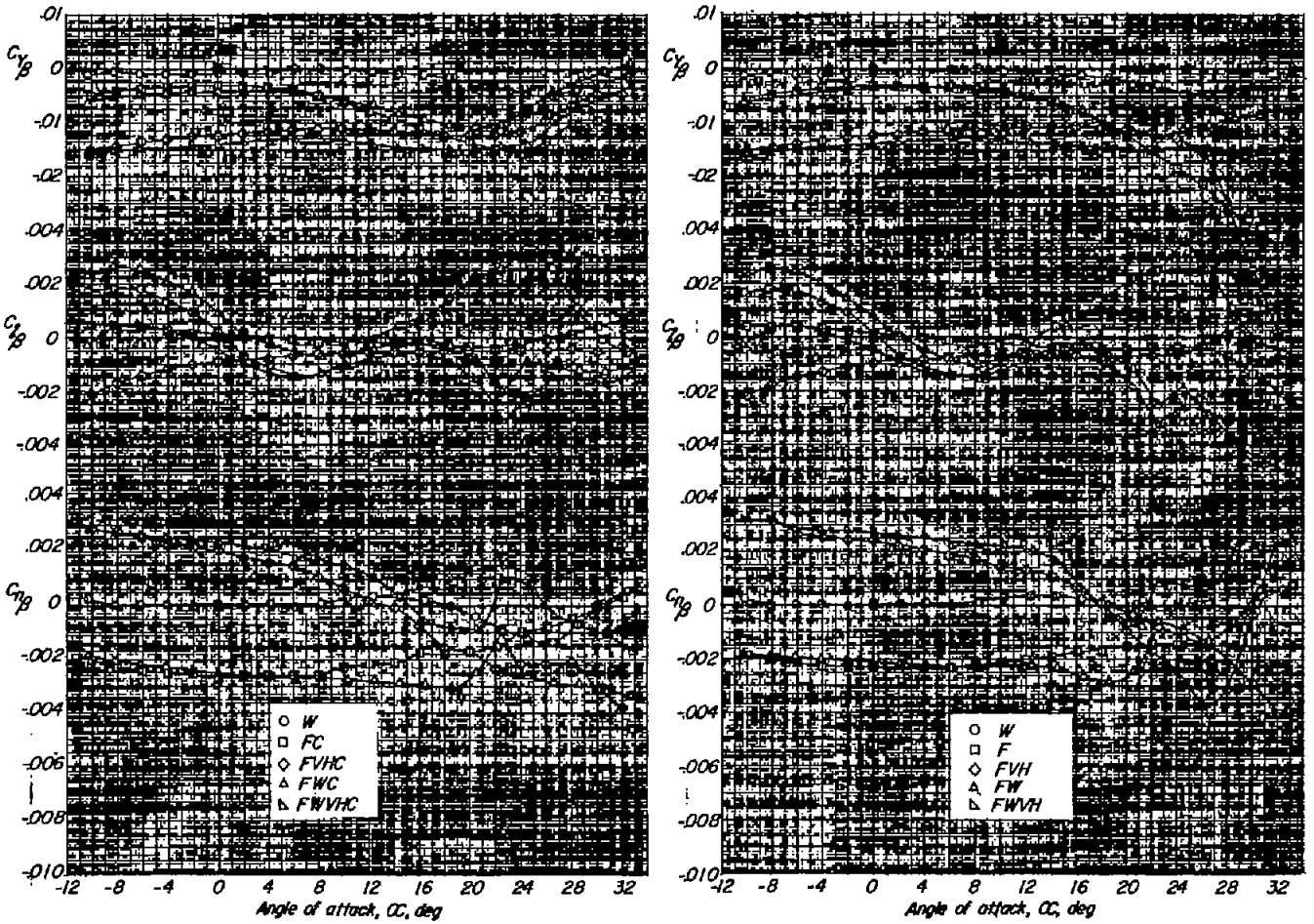

(a) Canopy on.

(b) Canopy off.

Figure 19.- Variation of C_{Y_β}, C_{l_β}, and C_{n_β} with α for the components of a 45° sweptback wing model having a pointed fuselage of fineness ratio 9.26.

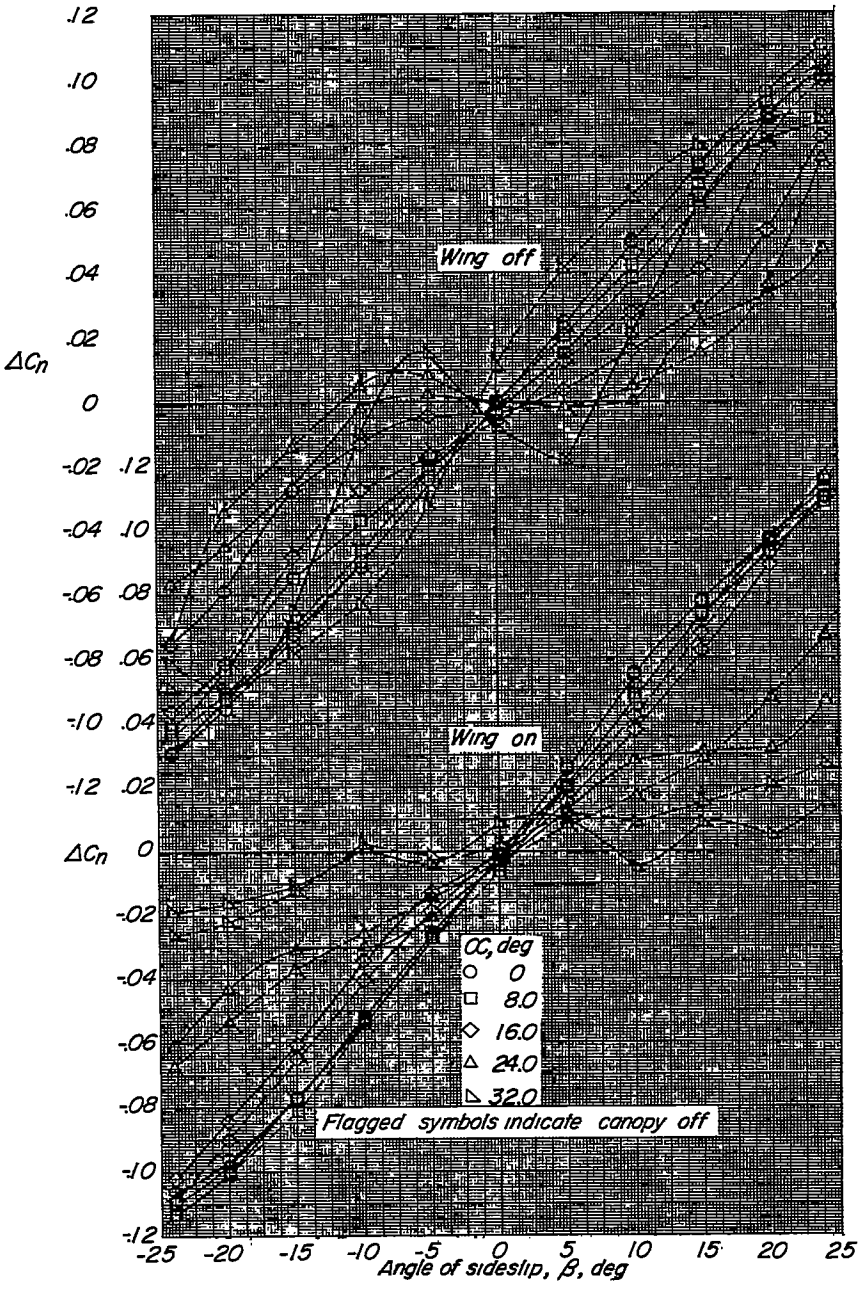

Figure 20.- Effect of canopy on the variation with angle of sideslip of the contribution of the tail assembly to the yawing-moment coefficient. Fuselage fineness ratio, 9.26; pointed nose; wing off and on.